LAPPEENRANTA UNIVERSITY OF TECHNOLOGY

LUT School of Engineering Science

Degree Program in Technical Physics

*Sergei Afanasev*

**Supercontinuum generation in photonic crystal fiber and its spectral dependence on the pump laser power**

Examiner: Professor, Erik Vartiainen

Supervisor: Professor, Erik Vartiainen

## ABSTRACT

Lappeenranta University of Technology

LUT School of Engineering Science

Degree Program in Technical Physics

Sergei Afanasev

## Supercontinuum generation in photonic crystal fiber and its spectral dependence on the pump laser power

This work is devoted to the study how different input laser powers will affect the supercontinuum spectra. At the moment there is not a lot of work on a similar topic and the more so no one with such a good resolution. For the experiment, a pulsed radiation source was used at a wavelength of 780 nm.

It is found that an increase in the pump power of the laser leads to a broadening of the spectrum and an increase in the radiation intensity. The rationale for these effects was proposed. In addition, for the first time in the world, measurements were made of a supercontinuum in a photonic crystal fiber with a resolution of 0.6 nm.

The results of supercontinuum studies at various powers are presented.

# Acknowledgements

# List of abbreviations and symbols

| | |
|---|---|
| $\theta_1$ | angle of incidence |
| $\theta_2$ | angle of refraction |
| $\theta_c$ | critical angle of incident |
| $\theta(\eta)$ | Heaviside single-step function |
| $c$ | speed of light in vacuum |
| $n$ | refractive index of a dielectric medium |
| $u$ | group velocity |
| $\beta$ | propagation constant |
| $\chi$ | electric susceptibility |
| $\mu_0$ | magnetic constant |
| $\nabla$ | nabla, first-order differential operator |
| $\omega$ | angular frequency |
| $\omega_0$ | central frequency |
| $\chi^{(3)}$ | third-order susceptibility |
| $\tilde{\chi}$ | Fourier transform of $\chi$ |
| $\Omega$ | frequency detuning |
| $\varepsilon_0$ | vacuum permittivity or electric constant |
| $a_j$ | attenuation coefficients |
| $\Phi(t)$ | nonlinear phase shift |
| $k_0$ | free-space wave number |
| $K$ | perturbation |
| $n_0$ | *linear* refractive index |
| $n_2$ | nonlinear refractive index |

| | |
|---|---|
| $I_0$ | peak intensity of light pulse |
| $I(t)$ | laser radiation intensity |
| $t$ | time |
| $\tau$ | pulse duration |
| A | envelope shape |
| F | force acting on a molecule |
| R | Raman part of the nonlinearity |
| S | spectrum of the pulse |
| P | polarization |
| W | interaction energy |
| XFROG | cross-correlation frequency-resolved optical gating |

| | |
|---|---|
| CARS | coherent anti-Stokes scattering |
| FWI | four-wave interaction |
| FWM | four-wave mixing |
| GVD | group velocity dispersion |
| LBO | lithium triborate |
| MS | microstructure |
| NIR | near-infrared |
| PCF | photonic crystal fiber |
| PSM | phase self-modulation |
| SC | supercontinuum |
| SRS | stimulated Raman scattering |
| USLP | ultrashort laser pulse |
| YLF | yttrium lithium fluoride |

# Contents

# 1  Introduction

Nonlinear optical interactions of ultrashort laser pulses (USLP) open the possibility of generating artificial white light with unique spectral properties, regulated by time duration and high spectral brightness. Materials and structures that make it possible to convert ultrashort laser pulses into supercontinuum radiation open new ways of solving optical communication problems and controlling extremely short light pulses. The supercontinuum generators based on microstructured fibers help to achieve record accuracy in optical metrological measurements and open the way for creating new compact multiplex sources for nonlinear spectroscopy, microscopy, and laser biomedicine. The study of the generation of white light in microstructured fibers makes it possible to observe new regimes of nonlinear-optical interactions of ultrashort laser pulses. New fiber structures and materials with large optical nonlinearities provide high efficiency of spectral and temporal transformation of ultrashort laser pulses and allow realizing methods for generating broadband radiation with controlled spectral, temporal and phase characteristics.

Three hundred years after Newton's experiments on the decomposition and the synthesis of white light, the nonlinear optical conversion of ultrashort laser pulses allowed to obtain artificial white light with interesting spectral properties, regulated by time duration and high spectral brightness. In view of the length and continuity of the spectrum, white light with such properties is often called supercontinuum (SC) radiation. Laser generation of white light is a unique physical phenomenon. It is used to solve problems of optical communication, controlling extremely short light pulses, helps to achieve record accuracy in optical metrological measurements, is used for the optical sounding of the Earth's atmosphere, and opens the way for creating new compact multiplex sources for laser biomedicine, nonlinear spectroscopy, and microscopy.

The present thesis is dedicated to laser generation of white light and the study of the effect on its properties on various parameters. It describes a detailed study of the supercontinuum process and methods for obtaining it. The thesis consists of 8 chapters. Chapter 4 gives the necessary background about supercontinuum generation mechanisms. Chapter 5 is devoted to the principles of light propagation in an optical fiber. In chapter 6 experimental technique and result of supercontinuum measurements are presented.

## 2 Nonlinear optics: fundamentals and applications

Nonlinear optics is a field of science that deals with studying the interaction of light fields with a medium where a nonlinear polarization $P$ is indiced by the incident electric field $E$. In most media, this nonlinearity is observed only at very high light intensities achieved by means of lasers. It is customary to consider both the interaction and the process itself to be linear if its probability is proportional to the first power of the radiation intensity. If this degree is greater than one, then both the interaction and the process are called nonlinear.

The appearance of nonlinear optics is associated with the development of lasers that can generate light with large electric field intensity commensurate with the intensity of the microscopic field in atoms. The main causes that cause differences in the effect of high-intensity radiation from low-intensity radiation on matter:

1) At a high radiation intensity, the main role is played by multiphoton processes, when several photons are absorbed in an elementary act;

2) At a high radiation intensity, self-action effects occur that lead to a change in the initial properties of the substance under the influence of radiation.

Significant advances in recent decades in nonlinear optics have been made possible by the use of artificial white light, also called supercontinuum emission. We are talking about the field of optics of ultrashort pulses, quantum optics, optical metrology, laser spectroscopy and laser biomedicine.

# 3   First steps in optics

Nonlinear optics is a field of science that deals with the study of the interaction of light fields with a substance that reacts via a nonlinear response to the incident fields. For many ages, the light emanating from the Sun was as one of the main instruments of experimental optics. Experiments performed directly with sunlight made it possible to establish a large number of geometric optics laws, such as the laws of reflection and refraction, to observe a number of fundamental optical phenomena, to identify the optical geometry of our vision.

Only 350 years ago, physicists began to associate sunlight with the richness of colours surrounding us, with the greatest brightness manifested in daylight. The light was colourless. Important works on the way to the formation of a physical understanding of colour understanding were the works of Descartes, who explained the origin of the rainbow, and Grimaldi, who observed the appearance of colour rings around a stain of sunlight passing through a pinhole on an opaque screen. Newton's experiments (Fig. 1a) proved for the first time the attendance of colour in the sunlight itself. White light was not the simplest form of radiation, acquiring colour due to illuminated and translucent objects, as was thought before, but a mixture of the whole variety of colours.

In 1928, sunlight helped Raman and Krishnan observe a "new type of secondary scattering" [1], which occurs when sunlight passes through liquids and gases. Investigations of this phenomenon, called Raman scattering, made it possible to understand the physical nature of the shift's frequency in the scattering of light by molecules and showed that the inflexible light scattering effect opens up unique possibilities for the spectroscopy of matter in the condensed and gas phases.

The revolutionary achievements in the field of laser spectroscopy, as well as significant advances in last decades in the field of optics of ultrashort pulses, nonlinear and quantum optics, and laser biomedicine, have become possible thanks to the use of artificial white light generated by laser sources (Fig. 1b), also called supercontinuum emission. The radiation spectrum of the supercontinuum can overlap the visible and small part of the IR range, which is hundreds of times wider than the monochromatic light transmitted through the fiber, generated by most lasers. According to its spectral brightness and intensity, white light generated by lasers is hundreds of thousands of times greater than the natural white light that comes from the Sun to our planet from.
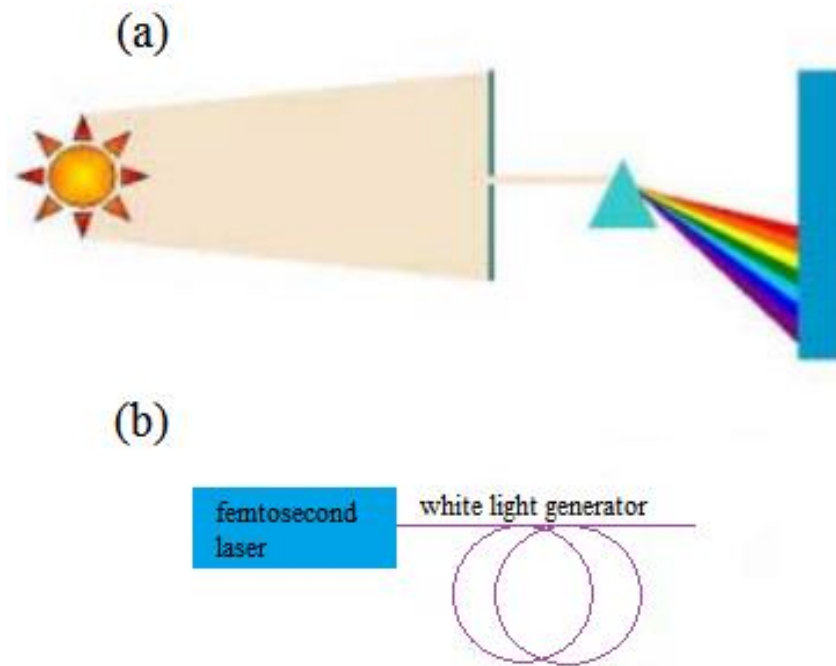
Figure 1: (a) Spectral components of white light in Newton's experiments. (b) White light generated as a result of a nonlinear optical conversion of ultrashort laser pulses.

# 4   Supercontinuum generation

## 4.1 Discovery and initial stage of investigation of supercontinuum generation

For the first time, laser radiation of white light is mentioned in the works of Alfano and Shapiro [2]. In the bulk of the borosilicate glass, they observed the spectral broadening of the picosecond laser pulse radiation of the second harmonic of a neodymium-garnet laser with an energy of about 5 mJ. At laser radiation intensity in the sample of the order of 1 GW/cm$^2$, radiation was generated in the wavelength range from 400 to 700 nm. Following the publication of Alfano and Shapiro, experimental studies have shown the possibility of generating a supercontinuum in materials of various structure and nature, such as gas media, inorganic and organic liquids, and solid materials. Following experiments performed with bulk samples, white light generation was also observed in the waveguide regime using quartz optical fibers. Experiments on laser generation of white light, performed 40 years ago, contributed to the development of the theory of time and spatial self-action of ultrashort laser pulses and stimulated the formation of new broadband radiation sources for spectroscopy and time-resolved measurements [3]. The generation of the supercontinuum was also used as a method of forming ultrashort pulses and was used to create multifrequency multiplex sources of radiation. In recent years, thanks to the appearance of new waveguide structures and the progress of laser technology, the generation of the supercontinuum has become widespread as a method for solving a wide range of fundamental and applied problems of ultrashort light pulses, breakthrough in optical metrology, remote analysis of the terrestrial atmosphere, laser biomedicine, microscopy and nonlinear spectroscopy.

## 4.2 Phase self-modulation (PSM) and elementary theory stage of spectral broadening of USLP

The key factor for the generation of a supercontinuum by a physical factor is the presence of an additive to the refractive index, depending on the intensity of the laser

radiation, in a medium with Kerr's nonlinearity [4]:

$$n = n_0 + n_2 I(t), \tag{4.1}$$

where $n_0$ is the linear refractive index of a medium, $n_2 = (\frac{2\pi}{n_0})^2 \chi^{(3)}$ is the nonlinear refractive index, $\chi^{(3)}$ is the third-order nonlinear optical susceptibility, and $I(t)$ is the laser radiation intensity.

The appearance of an intensity-dependent additive to the refractive index in the case of short laser pulses leads to modulation of the phase of the laser field-phase self-modulation. Taking into account expression (1), represent the nonlinear phase shift of a pulse passing a distance L in a medium with Kerr's nonlinearity in the next form

$$\Phi(t) = \frac{\omega}{c} n_2 I(t) L. \tag{4.2}$$

In accordance with expression (4.2), due to the dependence of the refractive index of the medium on the radiation intensity, the time dependence of the field intensity in the light pulse leads to a dependence of the nonlinear phase shift on time, which in turn leads to the appearance of a time-dependent deviation of the laser pulse frequency

$$\Delta\omega(t) = \frac{\omega}{c} n_2 L \frac{\partial I}{\partial t}. \tag{4.3}$$

The maximum spectral broadening of the pulse can be estimated as follows:

$$\Delta\omega(t) = \frac{\omega}{c} n_2 L \frac{I_0}{\tau}, \tag{4.4}$$

where $I_0$ is the peak intensity of light pulse, and $\tau$ is the pulse duration.

To get more exact expressions for the temporal envelope and the nonlinear phase shift induced by the PSM phenomenon, we use the theory of the PSM, based on the approximation of slowly changing amplitudes and taking into account the dispersion in the first order of the power-law decomposition of the propagation constant

$$\beta(\omega) \approx \beta(\omega_0) + u^{-1}(\omega - \omega_0), \tag{4.5}$$

where $\omega_0$ is the central frequency of the light pulse, and $u = (\frac{\partial \beta}{\partial \omega} \big|_{\omega=\omega_0})^{-1}$ is the group velocity.

The equation for the evolution of the slowly changing envelope $A(t, z)$ in these approximations is written in the next form [4]:

$$\frac{\partial A}{\partial z} + \frac{1}{u} \frac{\partial A}{\partial t} = i\tilde{\gamma}|A|^2 A, \tag{4.6}$$

$$\tilde{\gamma} = \frac{3\pi\omega}{2n_0^2 c} \chi^{(3)}, \qquad (4.7)$$

where $\tilde{\gamma}$ is the nonlinear coefficient.

In the accompanying coordinate system $z' = z$, $\eta = t - z/u$, equation (4.6) has a solution

$$A(\eta, z) = A_0(\eta)\exp(i\tilde{\gamma}|A_0(\eta)|^2 z), \qquad (4.8)$$

where $A_0(\eta)$ is the initial envelope shape.

The evolution of the nonlinear phase shift is described by the following expression:

$$\varphi_{nl}(\eta, z) = \gamma_{SPM} I_0(\eta) z), \qquad (4.9)$$

$$\gamma_{SPM} = \frac{2\pi n_2}{\lambda},$$

where $I_0(\eta)$ is the light pulse envelope.

The deflection of the instantaneous field frequency from the central frequency $\omega_0$ is given by the formula

$$\delta\omega(\eta, z) = -\frac{\partial \varphi_{nl}(\eta, z)}{\partial t} = -\gamma_{SPM} \frac{\partial I_0(\eta)}{\partial \eta} z. \qquad (4.10)$$

The momentum with quadratic dependence of the envelope on the traveling time

$$I_0(\eta) \approx I_0(0)\left(1 - \frac{\eta^2}{\tau_0^2}\right) \qquad (4.11)$$

acquires, as a result of the PSM, a linear chirp

$$\delta\omega(\eta, z) \approx 2\gamma_{SPM} \frac{I_0(0)}{\tau_0^2} \eta z. \qquad (4.12)$$

Such a chirp can easily be compensated with a prism system, chirped mirrors [5] or diffraction gratings to perform a temporary compressing of the laser pulse.

The spectrum of the pulse that experiences the PSM is written in the form

$$S(\omega) = \left| \int_0^\infty I(\eta) \exp(i\omega\eta + i\varphi_{nl}(\eta)) \, d\eta \right|^2. \qquad (4.13)$$

The temporary self-action of the light pulse leads to a symmetric broadening of its spectrum (Fig. 2). Nevertheless, even at moderate laser radiation intensities, there are a number of physical mechanisms that lead to asymmetry of the spectral broadening. The three most important mechanisms are related to spatial self-action, the formation of a shock front by the envelope, and the finite time of the nonlinear-optical response of the medium.
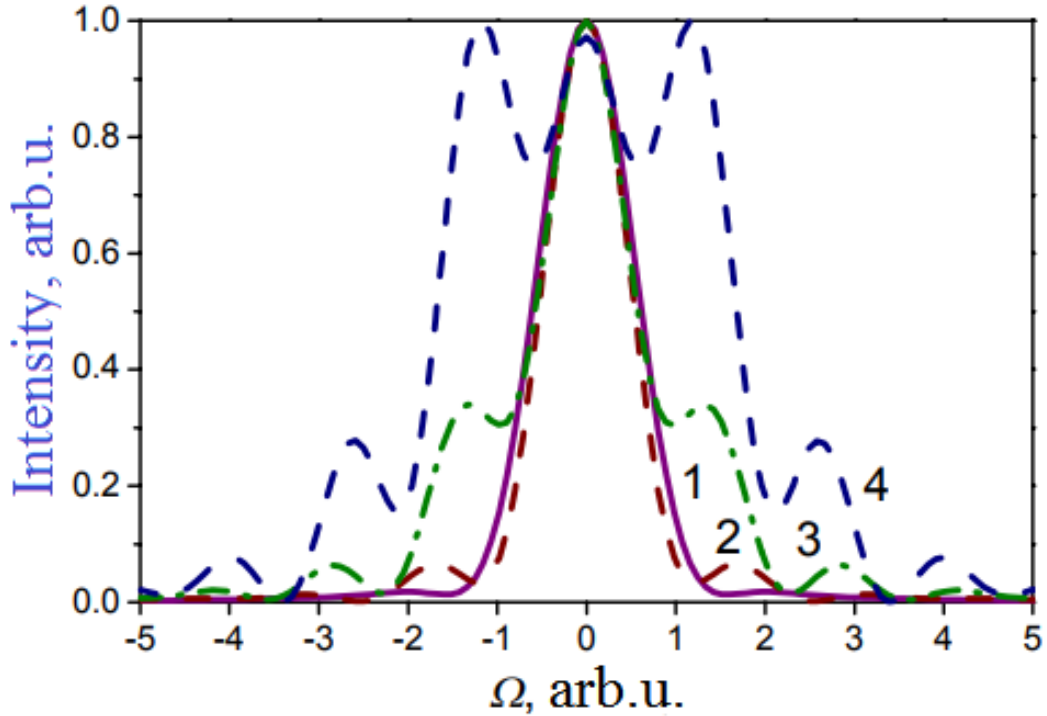
Figure 2: Laser pulse spectral broadening with an envelope of the shape of a hyperbolic secant and an initial duration of 30 fs in an optical fiber with a nonlinear refractive index $n_2$. Line 1 shows the initial spectrum. The initial pulse energy is (2) 0.1 nJ, (3) 0.2 nJ, (4) 0.3 nJ.

Spatial self-action [4] is related to the Kerr's nonlinearity of the medium. In the same way as the time profile of the intensity of the envelope of the laser field $I(t)$ leads to the modulation of the pulse phase, the nonuniformity of the intensity of the laser field in the beam $I(r)$ along the transverse coordinate $r$ forms a nonlinear lens, $n(r) = n_0 + n_2 I(r)$, which in turn leads to self-focusing or self-defocusing of the beam as a function of the sign of $n_2$. The increase in the intensity of laser radiation in a self-focusing beam leads to an increase in the efficiency of nonlinear optical interactions. As a rule, self-focusing is accompanied by an uncontrolled change in the intensity and phase of the laser pulse and leads to a complex spatial dynamics of the laser beam, one of the interesting manifestations of which is the decay of the laser beam into thin filaments. Due to the high intensity of laser radiation, filaments are sources of broadband optical radiation. The control of the properties of such radiation, however, is an intractable task. The formation of the shock front of the envelope of the light pulse [6, 7] is due to the dependence of the group velocity

of the pulse on the intensity. In a medium with $n_2 > 0$, nonlinearity leads to a positive additive to the group velocity. The rear edge of the pulse becomes steeper and the leading edge is more sloping. In the frequency representation, such a transformation of the light pulse leads to an asymmetry of its intensity spectrum. The maximum of the pulse spectrum shifts to the low-frequency region, and the short-wave part of the spectrum is considerably longer than the long-wave region.

The effects associated with the finite time of the nonlinear response of the medium, become observable for pulses of short duration [6]. The delay of the nonlinear response is equivalent to the dispersion of the nonlinearity of the medium in the frequency representation. A short pulse propagating in a medium with a delayed nonlinearity undergoes a low-frequency shift. The spectral broadening induced by the retarded nonlinearity is thus equivalent to Raman scattering.

## 4.3  Generation of the supercontinuum by the high-intensity laser pulses

An important direction of laser generation of white light is associated with the generation of a supercontinuum in the propagation of high-intensity femtosecond laser pulses in gas and liquid media. Laser radiation of high intensity leads to ionization of the medium. The free electrons that form as a result of ionization make an essential contribution to the nonlinear response of the gas and have a significant effect on the spectral, temporal and spatial dynamics of the laser pulse. In particular, the phenomenon of filamentation, observed during the propagation of high-intensity laser pulses in gas media, makes it possible to use the phenomenon of supercontinuum generation for remote sensing of the earth's atmosphere (Fig. 3) [8].
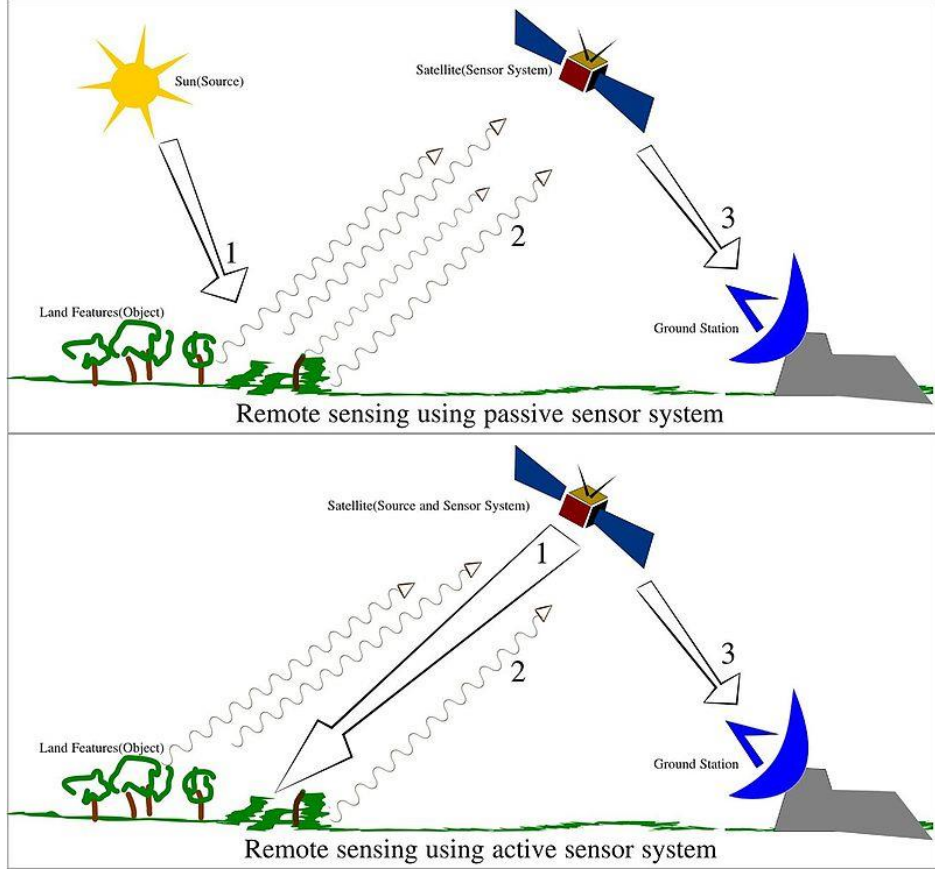
Figure 3: Passive remote sensing when the reflection of sunlight is detected by the sensor and active remote sensing when a signal is emitted by a satellite or aircraft and its reflection by the object is detected by the sensor.

Along with the effects of ionization, the effects of spatial self-action, the formation of the shock front of the envelope, the delayed nonlinearity of the medium, and the effects of high-order dispersion play an important role in the generation of the supercontinuum by high-intensity laser pulses. To account for all these phenomena, the equation for the slowly evolving field amplitude A normalized to the maximum field amplitude is written in the following form:

$$\left[i\frac{\partial}{\partial z} + \frac{1}{4}\left(1 - is\frac{\partial}{\partial \tau}\right)\nabla_\perp^2 - \frac{1}{4}\frac{L_{df}}{L_d}\left(\frac{\partial^2}{\partial \tau^2} + \frac{i}{3}\frac{L_d}{L_d'}\frac{\partial^3}{\partial \tau^3}\right)\right]A + L_{df}\left(1 + is\frac{\partial}{\partial \tau}\right) *$$

$$* \left(\frac{\Psi_{nl}}{L_{nl}} - \frac{|A|^4}{L_s}\right)A - \frac{L_{df}}{L_{pl}}\left(1 - is\frac{\partial}{\partial \tau}\right)N_e A + i\frac{L_{df}}{L_{MPA}}|A|^{2n-2}A = 0, \tag{4.14}$$

where $s = (\omega \tau_0)^{-1}$, $\tau_0$ is the initial pulse width, $\tau = t - z/u$ is the time in the accompanying coordinate system, $u = (\partial k / \partial \omega)^{-1}$ is the group velocity of momentum,

$k = \omega n_0/c$. The function $\Psi_{nl}$ takes into account both the instantaneous and delayed components of the nonlinearity

$$\Psi_{nl} = (1 - f_R)|A|^2 + f_R \int_{-\infty}^{\tau} R(\tau - \theta)|A(\theta)|^2 d\theta, \tag{4.15}$$

where $R(\eta)$ is the function describing the retarded (Raman) part of the nonlinearity of the medium, $f_R$ is the contribution of the Raman part of the nonlinearity to the intensity-dependent increment to the refractive index.

Equation (4.14) includes the following spatial scales: $L_{df} = kw_0^2/2$ – diffraction length, $w_0$ – radius of the laser beam; $L_d = \tau_0^2(2k_2)^{-1}$, $L_d' = \tau_0^3(2k_3)^{-1}$, $k_2 = \frac{\partial^2 k}{\partial^2 \omega}$, $k_3 = \frac{\partial^3 k}{\partial^3 \omega}$ – lengths at which the dispersion of a medium of the second and third orders is manifested. Length of nonlinear interaction $L_{nl} = c(\omega n_0 n_2 I_0)^{-1}$ is determined by the nonlinear refractive index $n_2$ and the peak intensity of the laser radiation $I_0$. At the characteristic length $L_s = c(\omega n_0 n_4 I_0^2)^{-1}$, self-focusing limitation (saturation) phenomena occur due to fifth-order nonlinearity ($n_4$ is determined by the fifth-order nonlinear susceptibility $\chi^{(5)}$). The lengths $L_{pl} = km_e c^2 (2\pi e^2 \tau_0 N_0 \sigma^{(n)} I_0^n)^{-1}$ and $L_{MPA} = n\hbar \omega N_0 \sigma^{(n)} I_0^{n-1}/2$ characterize the spatial scales on which the phenomena associated with the formation of plasma and multiphoton absorption due to ionization losses. Here $m_e$ and $e$ are the mass and charge of an electron, $N_0$ is the density of neutral particles, and $\sigma^{(n)}$ is the cross section for n-photon ionization. The electron density $N_e$ in equation (4.14) is normalized to the value $\tau_0 N_0 \sigma^{(n)} I_0^n$.

The function of the Raman response associated with the combination-active molecular rotations is modeled as a damped oscillator:

$$R(\eta) \propto \Theta(\eta) \exp\left(\frac{\eta}{\tau_1}\right) \sin\left(\frac{\eta}{\tau_2}\right), \tag{4.16}$$

where $\Theta(\eta)$ is the Heaviside single-step function.

Nonlinear optical phenomena accompanying the propagation of high-intensity pulses in the atmosphere make it possible to obtain radiation from a high energy supercontinuum. The supercontinuum spectrum generated by intense laser pulses in the atmosphere has a pronounced peak at the wavelength of the pump radiation. The effects of plasma defocusing, the limitation of spatial self-action due to multiphoton absorption, as well as phase mismatches of nonlinear optical interactions caused by dispersion, hamper the

production of more uniform and broader radiation spectra.

## 4.4 Four-wave interactions and soliton mechanisms of supercontinuum generation in optical fibers

Optical fibers provide long lengths of the nonlinear-optical interaction of laser pulses of sufficiently high intensity, allowing to lower the requirements for the laser radiation power necessary for generating a supercontinuum. The radiation intensity of the supercontinuum formed in optical fibers is lower than the intensity of white light generated by powerful focused laser pulses in gas media. However, optical fibers allow the emission of a supercontinuum with a spectrum overlapping most of the visible range or even the entire visible and part of the IR ranges when using pulses with a characteristic peak power on the order of a kilowatt. Optical fibers open up wide possibilities for controlling the process of white light generation and the formation of supercontinuum radiation with the required spectral and temporal parameters.

As shown by early experiments on supercontinuum generation in optical fibers [3], performed using pulses of picosecond and nanosecond duration, the spectrum of the laser pulse propagating along the fiber is enriched by cascade stimulated Raman scattering (SRS) and parametric four-wave interactions (FWI). The new spectral components that result from these processes are then broadened by phase self-and cross-modulation, merging and leading to the generation of radiation with a wide continuous spectrum at the fiber output.

Four-wave interaction in optical fibers leads to a parametric transformation of pump fields with frequencies $\omega_{p1}$ and $\omega_{p2}$ with the generation of light fields at frequencies $\omega_a$ and $\omega_s$. High FWI efficiency is achieved under the conditions when the law of conservation of momentum (the phase-matching condition) $\beta_{p1} + \beta_{p2} = \beta_a + \beta_s$ is fulfilled simultaneously with the energy conservation law $\omega_{p1} + \omega_{p2} = \omega_a + \omega_s$ for the propagation constant $\beta_{p1}, \beta_{p2}, \beta_a, \beta_s$ of the waveguide modes of the fields with frequencies $\omega_{p1}, \omega_{p2}, \omega_a, \omega_s$, participating in FWI. For the FWI process, degenerate with respect to the pumping frequency, $\omega_{p1} = \omega_{p2} = \omega_p$, $\omega_a = \omega_p + \Omega$, $\omega_s = \omega_p - \Omega$, the

phase matching condition

$$2\beta(\omega_p) = \beta(\omega_p + \Omega) + \beta(\omega_p - \Omega),$$ (4.17)

is most simply satisfied in the region of anomalous dispersion near the wavelength corresponding to the zero group velocity dispersion (GVD). We represent the propagation constants of the waveguide modes at the Stokes and anti-Stokes frequencies $\omega_s$ and $\omega_a$ in the form of power series

$$\beta(\omega_s) \approx \beta_0(\omega_p) - \frac{1}{u_p}\Omega + \frac{1}{2}\beta_2(\omega_p)\Omega^2 + 2\gamma P,$$ (4.18)

$$\beta(\omega_a) \approx \beta_0(\omega_p) + \frac{1}{u_p}\Omega + \frac{1}{2}\beta_2(\omega_p)\Omega^2 + 2\gamma P,$$ (4.19)

where P is the peak power of the pump pulse, $\beta_0(\omega_p)$ is the propagation constant at the pump frequency in the absence of a nonlinear field-induced nonlinear addition to the refractive index (when P = 0), $u_p = \left(\frac{\partial\beta}{\partial\omega}\big|_{\omega=\omega_p}\right)^{-1}$ is the group velocity of the pump pulse, $\beta_2(\omega_p) = \frac{\partial^2\beta}{\partial^2\omega}\big|_{\omega=\omega_p}$,

$$\gamma = (n_2\omega_p)/(cS_{eff}),$$ (4.20)

- nonlinear coefficient, $S_{eff} = \left[\int_{-\infty}^{\infty}\int_{-\infty}^{\infty}|F(x,y)|^2dxdy\right]^2/\int_{-\infty}^{\infty}\int_{-\infty}^{\infty}|F(x,y)|^4dxdy$ is the effective area of the mode with the transverse profile of the field $F(x,y)$.

Taking into account the expression for the constant propagation of the pump pulse

$$\beta(\omega_p) = \beta_0(\omega_p) + \gamma P$$ (4.21)

the condition of phase matching (4.17) leads to the following relation:

$$\beta_2(\omega_p)\Omega^2 + 2\gamma P = 0$$ (4.22)

The relation (4.22) can be satisfied only for $\beta_2(\omega_p) < 0$ ; in the region of anomalous dispersion. Due to this circumstance, supercontinuum sources based on standard optical fibers, as a rule, most effectively convert near-infrared radiation, but do not allow, however, to provide high output radiation intensities in the visible part of the spectrum. This is due to the fact that the zero GVD for standard optical fibers, as a rule, lies near the wavelength $\lambda_z = 1.3 \ \mu m$. The phase matching region (4.17) for FWI processes under these conditions is limited by a small frequency interval in the infrared range. Another important mechanism for generating a supercontinuum in standard optical fibers is associated with

stimulated Raman scattering. This mechanism leads to a preferential broadening of the spectrum into the long-wave (Stokes) region. Under the conditions of standard optical fibers, stimulated Raman scattering also does not lead to a significant enrichment of the visible part of the spectrum of the supercontinuum.

The supercontinuum generation in optical fibers is interest for the development of multifrequency radiation sources for frequency multiplexing in fiber-optic communication lines. For this purpose, it is required to ensure high efficiency of generation of broadband radiation with a sufficiently flat spectrum and low noise level for pulses following with gigahertz repetition frequencies. One of the promising approaches to solving this problem is to use adiabatic compression of solitons in the anomalous dispersion regime in a fiber with a length-changing GVD [9]. Another interesting solution is based on the use of spectral broadening of laser pulses due to the PSM mechanism in the normal dispersion mode [7]. To reduce the influence of effects associated with the temporary spreading of light pulses, special fibers with low values and a shallow profile of the GVD are used.

# 5 Laser generation of white light in MS fiber

## 5.1 Basic principles of light propagation in optical fiber

The propagation of light through the fiber can be explained on the basis of the principle of total internal reflection (TIR) (Fig. 4), which follows from Snell's law of refraction (5.1).
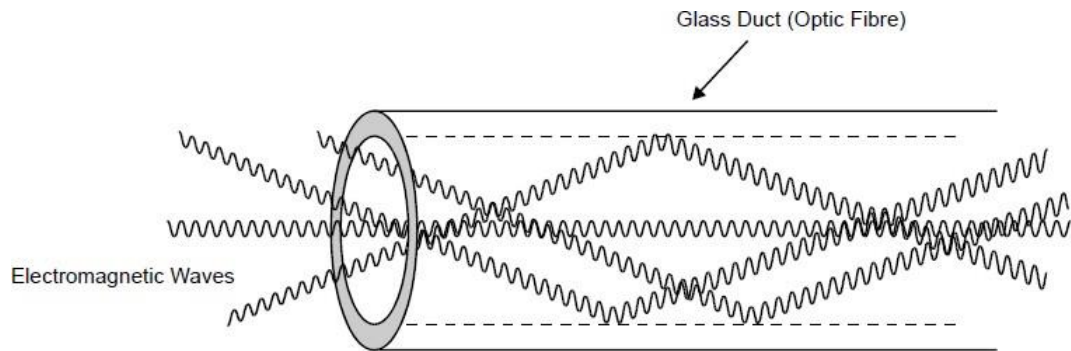


Figure 4: The propagation of electromagnetic waves in an optical fiber

$$\frac{sin\theta_1}{sin\theta_2} = \frac{n_2}{n_1} \tag{5.1}$$

where $n_1$ is the refractive index of the core, $\theta_1$ is the angle of incidence, $n_2$ is the refractive index of the cladding, and $\theta_2$ is the angle of refraction.

When a ray passes through the interface between two media with different refractive indices, refraction occurs. In addition, a small amount of incident light is reflected back. If a ray travels from a dielectric with higher refractive index $n_1$ at an angle $\theta_1$ to the normal, then in a medium with lower refractive index $n_2$ the ray will travel at an angle $\theta_2$, where $\theta_2$ is greater than $\theta_1$ (Fig. 5).
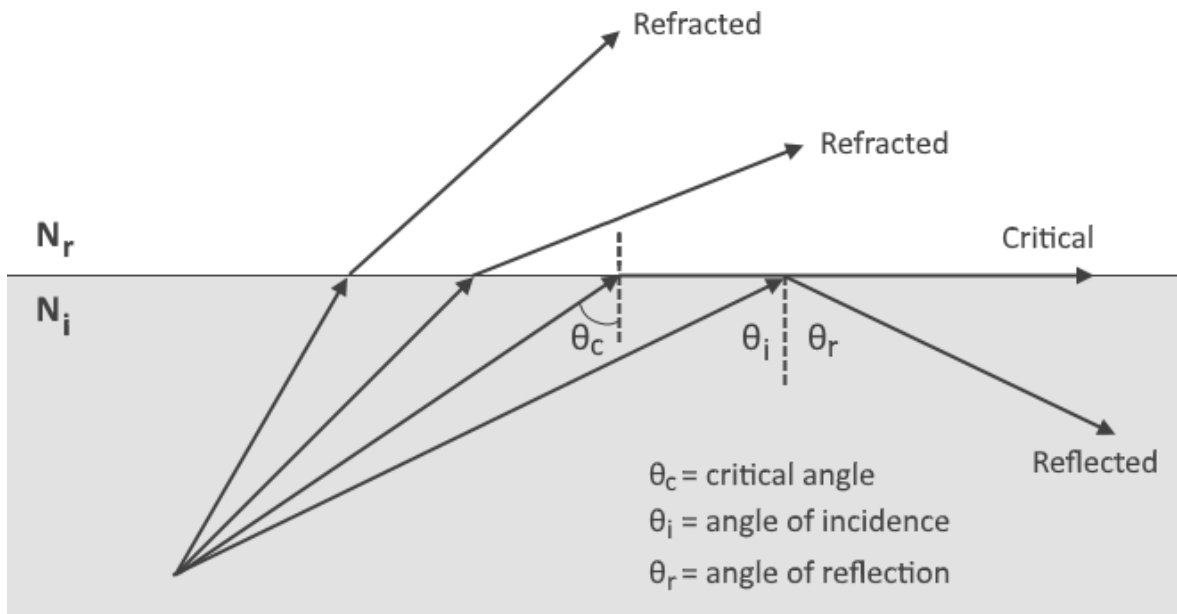
Figure 5: Ray refraction.

## 5.2 Microstructured fiber: methods for controlling dispersion and nonlinearity

Microstructured fibers [10] are waveguide structures of a new type. Unlike typical optical fiber (Fig. 6a), consisting of a core with a refractive index $n_{core}$ and a cladding with a refractive index of $n_{cladding}$, the MS fibers are a quartz or glass microstructure with a periodically or aperiodic system of cylindrical air holes oriented along the fiber axis (Fig. 6b). Such a microstructure is usually manufactured by drawing at high temperature from a preform made from hollow capillaries.

A microstructure defect that corresponds to the absence of one or more air holes (in the centre of the structure in Fig. 6b) serves as the core of the fiber, providing a waveguide mode of propagation of electromagnetic radiation. In standard fibers, a complete internal reflection is provided when the condition $n_{cladding} < n_{core}$. Waveguide modes of electromagnetic radiation in MS fibers are formed as a result of interference of reflected and scattered waves. The introduction of the effective refractive index $n_{eff}$ ($n_{eff} = \beta_f c/\omega$) for the MC cladding, allows us to write down the condition for the existence of waveguide modes in the core of the fiber formed by the microstructure defect (Fig. 6b)

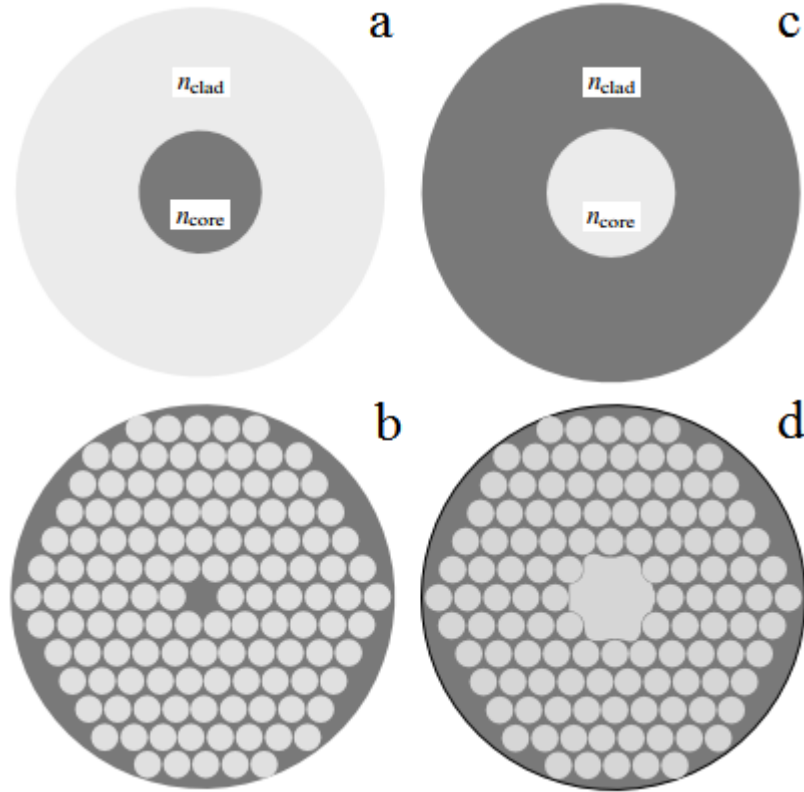similar to the condition for the existence of total internal reflection in a standard fiber: $n_{eff} < n_{core}$ .
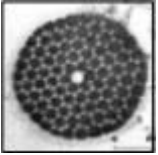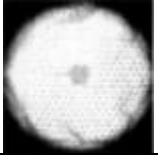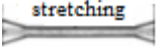


Figure 6: Optical fibers of different architecture: (a) standard optical fiber consisting of a core with a refractive index $n_{core}$ and a cladding with a refractive index $n_{cladding}$ ; (b) MS fiber; (c) standard hollow fiber with a continuous cladding; (d) hollow fiber with a PC cladding.

Along with the usual waveguide regimes provided by the phenomenon of total internal reflection, under certain conditions, the MC fibers support waveguide modes of electromagnetic radiation, formed due to the high reflectivity of the envelope in the region of photonic forbidden bands [11]. Such waveguiding modes implemented in fibers with a shell in the form of two-dimensionally periodic microstructure (two-dimensional photonic crystal) and a hollow core (Fig. 6d). The photonic band gap arising in the transmission spectrum of a two-dimensional periodic shell of a given type provides a high reflection coefficient for radiation propagating along the hollow core, allowing nature to reduce the optical losses inherent in the modes of ordinary hollow waveguides (Fig. 6c) with a

continuous envelope and rapidly growing with a decrease in the diameter of the hollow core.

Table 1. Atlas of MS-fiber

| Type of fiber | Characteristic fiber structure | Mechanism of formation of waveguide modes | Application | | | | | |
|---|---|---|---|---|---|---|---|---|
| | | | Telecommunications | Metrology | Ultrashort pulses | Nonlinear optics | Laser physics | Biomedicine and photochemistry |
| MC-fiber with quartz or glass core |  | Total internal reflection | An acceptable level of losses has been reached | Generation of frequency combs with a width more than an octave for a femtosecond clock | Compression and phase measurement, GVD control, solitons | Increase in the efficiency of PSM, FWI, SRS, generation of SC | New schemes of fiber lasers | Optical coherence tomography |
| Hollow PC fiber |  | Photonic forbidden zones of the FC cladding | If losses are reduced | | Transmission in the region of maximum transmission | Increase in the efficiency of PSM, FWI, SRS | | Transmission of laser pulses for laser dentistry |
| MC-integrated waveguide channels |  | Total internal reflection | Multiplex frequency conversion | | GVD control, solitons | FWI in pump depletion mode | Highly efficient frequency conversion of femto-second pulses | Initiation of photochromatism |
| Over-stretched fibers |  | Total internal reflection | Couplers, multiplexers, demultiplexers | Generation of frequency combs with a width more than an octave for a femtosecond clock | GVD control, solitons | Increase in the efficiency of PSM, FWI, generation of SC | New schemes of fiber lasers | Optical coherence tomography |

Microstructured fibers have a number of unique properties that open up new possibilities for the transmission of electromagnetic radiation over long distances [10], as well as for the nonlinear optical conversion of laser pulses [12]. The uniqueness of MS fibers for laser physics, nonlinear optics, and optical technologies is due to the ability to control the dispersion of waveguide modes due to a change in their structure and a high degree of localization of electromagnetic radiation in the core of microstructured fibers associated with a significant difference in the refractive index of the core and an effective refractive index of a microstructured shell. Controlling the dispersion properties of waveguide modes opens up new possibilities in the field of optical telecommunications and optics of ultrashort pulses. A high degree of localization of radiation in the core of the fiber leads to a radical increase in the efficiency of nonlinear optical interactions and makes it possible to observe new nonlinear optical phenomena.

To date, several types of MC fibers have been developed and are successfully used, which make it possible to solve a wide range of problems of nonlinear optics, optical metrology, laser physics, and biomedical optics (table 1) [10]. MS-fibers with a large difference in the refractive index of the core and the effective refractive index of the shell make it possible to achieve a high degree of localization of the electromagnetic field in the core, which leads to high values of the nonlinearity coefficient $\gamma$ (expression (4.20)) responsible for the efficiency of nonlinear optical interactions. An increase in the efficiency of nonlinear-optical interactions and the possibility of controlling the dispersion properties of waveguide modes opens the possibility of using low-energy laser pulses, including non-amplified laser pulses, for controlled supercontinuum generation [13, 14]. The spectral width of the supercontinuum emission under certain conditions can be several octaves.

Control of the dispersion of waveguide modes allows solving the phase matching problem for four-wave interaction processes [15]. Microstructured fibers are therefore used not only as sources of broadband radiation but also as frequency converters for laser pulses [12].

The different architecture of the MS fibers allows one to achieve large values of the birefringence parameter. In such fibers, it is possible to realize the polarization control of the supercontinuum generation phenomenon and the frequency conversion of laser pulses, and to realize the polarization demultiplexing of the supercontinuum radiation, separating out regions of the spectrum with different polarization from broadband radiation.

To create fiber-optic lasers and amplifiers, and also to develop a new class of optical

sensors [16,17], fiber with a double MC cladding are of considerable interest. In MC-fiber lasers, the inner part of the cladding provides a single-mode regime and a large area of the waveguide mode for obtaining high laser radiation power. The outer part of the cladding localizes the pump radiation in the inner part of the MC fiber. In MC-fiber sensors, the exciting radiation is delivered to the object by the core. The inner part of the envelope serves to deliver the scattered or fluorescent signal in the opposite direction along the fiber to the radiation receiver, which can be located next to the radiation source [16]. Such a fiber design provides high efficiency of sounding chemical and biological solutions by single-photon and two-photon luminescence methods. Radiation propagating along the core of the fiber causes luminescence of the detected molecules [17]. Thus, fiber sensors can be integrated into storage and processing systems for chemical and biological data, including biochips, to read and convert stored information.

The periodicity of the location of air holes in the fiber sheath is a key factor for the formation of waveguide modes in MS fiber with a hollow core [11]. A characteristic feature of a two-dimensional periodic structure (two-dimensional photonic crystal) of a cladding of such a fiber is the presence of photonic forbidden bands-regions of frequencies in which the structure is characterized by a high reflection coefficient. Hollow PCF open up unique opportunities for improving the efficiency of nonlinear-optical interactions in the gaseous phase, including stimulated Raman scattering, FWI, coherent anti-Stokes Raman scattering (CARS). Such fibers can also be used to create compressors, switches, limiters, and diodes for high-power laser pulses. Hollow PCF is used to transmit high-power laser radiation for the purpose of microprocessing materials and laser biomedicine. The phenomena of time and spatial self-action of high-power laser pulses in hollow PC waveguides lead to the formation of temporal solitons. On the basis of hollow PCF, new gas cuvettes compatible with fiber technologies are created to effectively convert the radiation frequency of nonlinear spectroscopy.

## 5.3 Nonlinear optical interactions of ultrashort pulses in MS fibers

The generation of a supercontinuum in MS fibers is of interest as a complex physical phenomenon and as a way of creating new effective sources of broadband radiation [13, 14]. The key advantages of MC fibers as white light generators and frequency converters

are associated with the possibilities of actively forming the waveguide mode dispersion profile and controlling the optical nonlinearity by changing the structure of the MC fiber [10]. The unique dispersive properties of MC fibers allow one to observe new nonlinear optical phenomena such as suppression of the soliton frequency shift, third harmonic generation at a frequency different from the tripled pumping frequency, scalar and vector modulation instabilities of new types. A certain type of MC-fiber structure allows to achieve a shift of the point of zero GVD to the region of 750-800 nm. Fibers of this class allow observing interesting soliton phenomena for femtosecond pulses of a sapphire titanate laser and provide high efficiency of nonlinear-optical conversion of such pulses, including the possibility of efficient generation of spectral components in the visible part of the spectrum.

## 5.4 Modulation instability of femtosecond pulses in MS fiber

For a wide class of nonlinear systems of physical, chemical and biological nature, the phenomenon of modulation instability is characteristic. The instability of this type leads to a change in the character of the wave process under conditions of simultaneous action of nonlinearity and dispersion of the medium and the formation of a pulse-spike structure in a temporal or spatial representation. Modulation instabilities are observed in hydrodynamics, nonlinear optics, plasma physics, and are also characteristic for a matter in the Bose-Einstein condensation state.

In nonlinear optics, the modulation instability manifests itself in the transformation of the spectrum, the time shape, and the spatial profile of the laser radiation [7]. High values of the gain factors of new frequency components that appear in the laser radiation spectrum as a result of modulation instability are achieved in optical fiber [7], which provide long lengths of nonlinear-optical interaction.

The simplest mode of modulation instability for the pulsed regime of nonlinear optical interactions in an optical fiber can be explained on the basis of relations (4.17), (4.21) expressing the phase matching condition for the parametric FWM process $2\omega_p = \omega_a + \omega_s$. The generation efficiency of the Stokes and anti-Stokes components, according to the relation (4.22), is especially effective when the central frequency of the pump pulse lies in

the region of the anomalous dispersion, $\beta_2(\omega_p) < 0$, and the frequency detuning $\Omega$ satisfies the equality

$$\Omega = \pm(\frac{2\gamma P}{|\beta_2(\omega_p)|})^{1/2} \qquad (5.2)$$

The phenomenon of modulation instability in MC fiber provides high efficiency of laser frequency conversion, while the fiber itself, operating in the modulation instability mode, can serve as an effective source of correlated photon pairs. In Fig. 7 shows a characteristic spectrum of laser radiation transformed due to the scalar modulation instability in the MS fiber [18]. Pulses were obtained from a titanium-sapphire laser with the energy of 0.1-1.0 nJ. The pulse length was 50 fs, the central wavelength 795 nm, and the repetition rate 10 MHz. The radiation was introduced into one of the lateral microchannels of the MC fiber with the cross-sectional structure shown in the inset to Fig. 7.
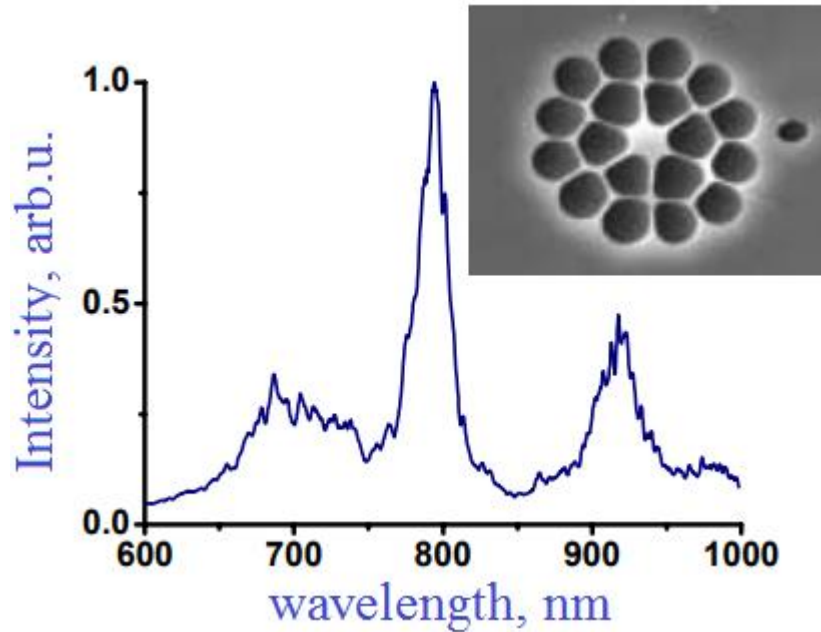


Figure 7: Generation of lateral components in the spectrum of the laser pulse of radiation from titanium-sapphire laser transmitted through the MC fiber with the cross-sectional structure shown in the inset. The initial duration of the laser pulse is 50 fs. The energy at the entrance to the fiber is 0.5 nJ.

In the emission spectrum recorded at the output of the MC fiber, intense Stokes and anti-Stokes components are observed. The experimental results thus indicate the possibility of using modulation instability for efficient frequency conversion and parametric

amplification of femtosecond laser pulses, and also for the creation of efficient and compact fiber-optic sources of correlated photon pairs.

## 5.5 Parametric frequency conversion of ultrashort light pulses

Consider the phenomenon of cross-modulation instability for a two-frequency field of the form

$$E(x, y, z, t) = F(x, y) \sum_{j=1}^{2} A_j(z, t) \exp(i(B_j z - \omega_j t)), \qquad (5.3)$$

where $F(x, y)$ is the transverse field profile, $A_j(z, t)$ is the time pulse envelope, $B_j$ is the propagation constant, and $\omega_j$ is the center frequency, $j = 1, 2$.

The approximation of slowly varying amplitudes leads to the following equations for the evolution of the pump pulse (j = 1) and the test field (j = 2) [19]:

$$\frac{\partial A_j}{\partial z} + \frac{1}{2}\alpha_j A_j + (-1)^{j-1}\delta\frac{\partial A_j}{\partial \tau} + \frac{i}{2}\beta_{2j}\frac{\partial^2 A_j}{\partial \tau^2} = i\gamma_j(|A_j|^2 + 2|A_{3-j}|^2)A_j, \qquad (5.4)$$

$$\tau = t - \frac{z}{v_g}, \overline{v_g} = \frac{v_{g1}^{-1} + v_{g2}^{-1}}{2}, \delta = \frac{1}{v_{g2}} - \frac{1}{v_{g1}}, \beta_{2j} = \left(\frac{\partial^2\beta_j}{\partial\omega^2}\right)_{\omega=\omega_f}, \gamma_j = \frac{n_2\omega_j}{cS_j},$$

where $\alpha_j$ is the attenuation coefficients at the frequencies of the pump fields and the test field, $v_{gj}$ are group velocities of the pump pulse and the probe pulse, $n_2$ is the nonlinear refractive index of fiber material, and $S_j$ are effective areas of the waveguide modes of the pump field and the test field.

The dispersion relation for the wave number of the perturbation K [19]:

$$\left((K - \frac{\Omega\delta}{2})^2 - h_1\right)\left((K + \frac{\Omega\delta}{2})^2 - h_2\right) = C^2, \qquad (5.5)$$

$$h_j = \frac{1}{4}\beta_{2j}^2\Omega^2\left(\Omega^2 + \frac{4\gamma_j P_j}{\beta_{2j}}\right), C = 2\Omega^2\sqrt{\beta_{21}\beta_{22}\gamma_1\gamma_2 P_1 P_2}.$$

The amplification of the instabilities of the pump field and the test field is due to the parametric four-wave interaction with the wave synchronism induced by the phase-modulation phenomenon. The gain of parametrically generated spectral components is determined by the expression

$$G(\Omega) = 2Im(K), \qquad (5.6)$$

In Fig. 8a and 8b show the dependences of the group velocities and the dispersion of the group velocity on the wavelength, calculated for the waveguide modes (shown in the

insets to Fig. 8a) for the fiber. For the main waveguide mode, the emission wavelength of the chromium-forsterite laser (1240 nm) used as the pump field lies in the region of anomalous dispersion. The wavelength of the second harmonic of this laser (620 nm), serving as a test field, lies in the region of normal dispersion. The group delay of the pump pulse and the probe pulse in such a fiber is $\delta = 20\ ps/m$.
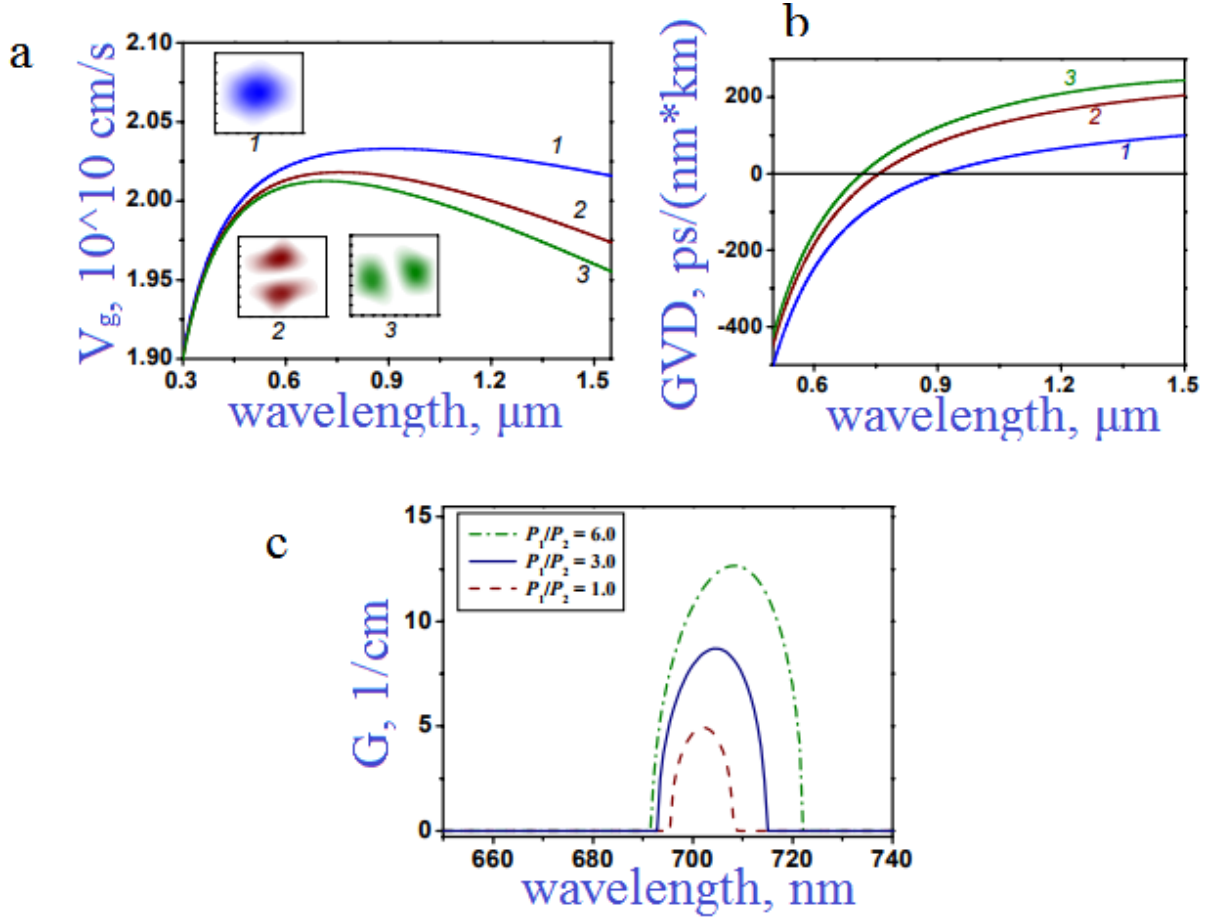


Figure 8: Group velocity (a) and dispersion of group velocity (b) for three waveguide modes (1 - 3) of a microstructured fiber with the cross-sectional structure shown in the inset to Fig. 7. The field intensity profiles in waveguide modes $1-3$ are shown in the inset to Fig. 8a. (c) The gain of the cross-modulation instability as a function of the wavelength of the radiation at various power-field ratios of the pump field P1 and the test field P2 for a fiber with the cross-sectional structure shown in the inset to Fig. 7.

In Fig. 8c shows the gain of the cross-modulation instability of the test field with a central wavelength of 620 nm in the fiber. This indicates the possibility of achieving high efficiency of parametric frequency conversion of the test field. The tuning of the wavelength of the parametric signal is achieved by varying the group delay parameter and

the power ratio of the pump field P1 and the test field P2. When the ratio P1 / P2 varies from 1 to 6, the wavelength corresponding to the maximum value of the gain G of the parametric signal at a fixed value of the group detuning ($20\,\mathrm{ps/m}$) moves in the region 703 - 714 nm

The laser system used in the experiments [20] consisted of a Cr: forsterite, stretcher, an optical isolator, a regenerative amplifier, a compressor and a crystal for doubling the frequency. A fiber ytterbium laser was used to pump the master laser. The master laser generated pulses with a characteristic duration of 50 to 70 fs and a repetition rate of 120 MHz. The central wavelength of these pulses was 1250 nm. The average radiation power of the laser was about 180 mW. The amplification of the femtosecond pulses generated by the master oscillator was performed by means of a regenerative amplifier pumped by the radiation of an Nd: YLF laser. Compression of laser pulses, amplified to an energy of the order of 100 μJ, was performed in a lattice compressor, which provided the duration of output pulses in the range $50 - 150$ fs. The frequency of chromium-forsterite laser radiation was doubled with an LBO crystal.

In the experiments, pump pulses and a trial field with an initial duration of about 100 fs were used. The energy of the probe pulse was fixed at a level of 2 nJ. The energy of the pump pulse varied from 1 to 50 nJ. The fiber length was 5 cm. At low pump radiation energies, the probe pulse experienced only a slight broadening (Fig. 9a) due to phase self-modulation in a MS fiber. An increase in the energy of the pump radiation led to appreciable changes in the spectrum of the probe pulse at the output of the fiber (Fig. 9b-9f). The low-frequency component that appears in the spectrum of the probe pulse at the fiber output, at pump pulse energy of 14 nJ, has a central wavelength of about 700 nm (Fig. 9b-9f). It is in this spectral region, according to the calculations, that the maximum gain G is reached.
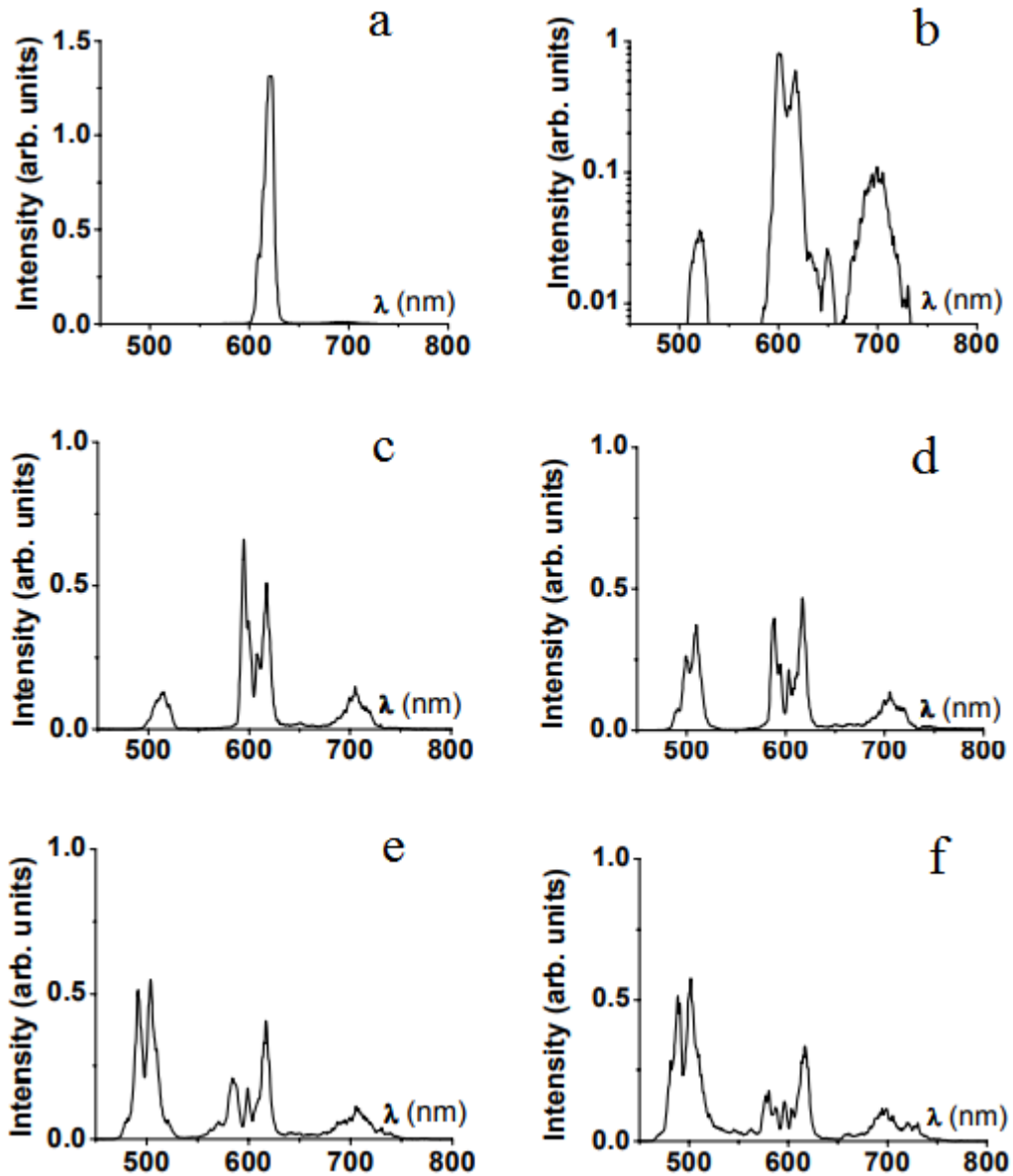
Figure 9: Spectra of the test field at the output of a MS fiber 5 cm long. The power of the pump pulses is (a) 3, (b) 7, (c) 30, (d) 42, (e) 70, (f) 100 kW. Power of the test field - 8 kW

As the power of the pump field is increased, a smooth tuning of the frequencies and amplitudes of the lateral spectral components is observed (Fig. 9b-9f). Thus, the characteristics of the phenomenon of parametric generation of side components in the spectrum of the probe femtosecond pulse in the field of the associated pump pulse in MS fibers are described in the framework of the standard model of cross-modulation instability. Control of the amplitude and frequency shift of the side components generated in the spectrum of the test field at the output of the fiber due to the parametric four-wave is obtained by changing the intensity of the pump field.

# 6 Fiber optic applications

## 6.1 The generation of white light and the revolution in optical metrology

The use of MC fibers in optical metrology systems is one of the most striking applications of fibers of this type. Thanks to the MC fibers in optical metrology, revolutionary changes took place that led to a significant simplification of laser systems used in optical metrology. From technically complex multistage complexes of the system of optical metrology and high-precision spectroscopy in the last decade have turned into compact desktop devices that provide unprecedentedly high accuracy of optical measurements.

The key idea is to use frequency combs, formed by femtosecond lasers operating in the mode-locking mode, to measure frequency intervals (Fig. 10). Femtosecond laser sources with synchronized modes provide generation of light pulse sequences separated by a time interval T equal to the bypass time of the laser oscillator pulse. In the spectral representation, such pulse sequences correspond to equidistant frequency combs (Figure 10) with the total spectral width determined by the pulse duration in the train and the frequency interval $\Delta\omega$ between the nearest spectral components. Such a frequency comb can be calibrated using an atomic frequency standard and used as a "line" for measuring spectral, and therefore temporal and spatial intervals. The transition from the usual wavelength measurement to optical spectroscopy to the measurement of frequency intervals by frequency combs makes it possible to increase the accuracy of optical measurements by many orders and to create a new generation of frequency and optical clock standards.

The idea of using laser sources of ultrashort pulses operating in the mode-locking mode for high-precision optical measurements was made almost 50 years ago. The work of the Hansch group [21] was the first to demonstrate experimentally the possibility of measuring the fine structure of atomic energy levels with the help of frequency combs formed by picosecond lasers with synchronized modes. In view of the relationship between the pulse width and the spectral width of the frequency comb, picosecond lasers do not allow a sufficiently wide range of measurements to be provided - the picosecond 'frequency ruler' is too short for this. For the wide practical use of frequency combs in optical metrology, sources of shorter, femtosecond laser pulses were required, and the direct attachment of

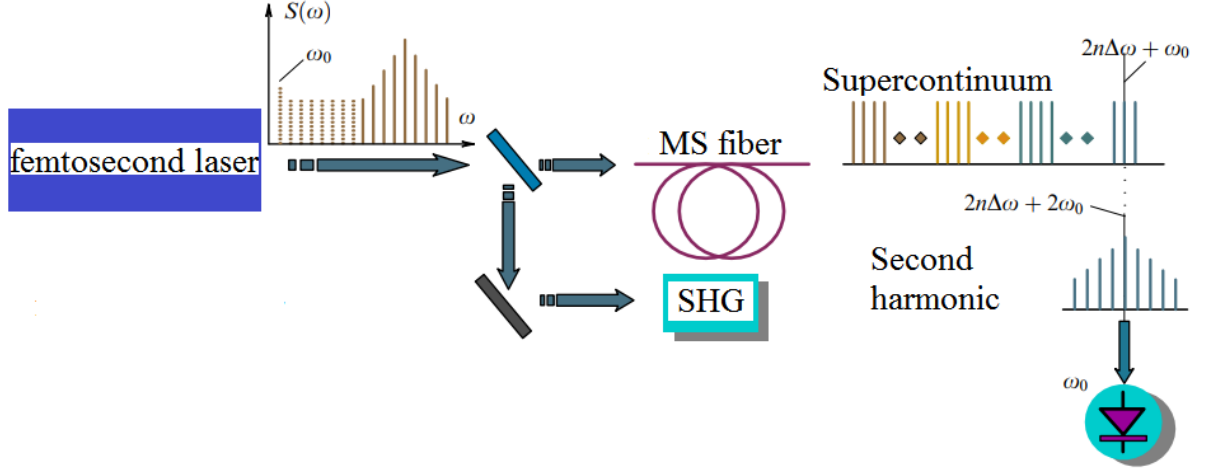such combs to atomic frequency standards became possible with the advent of MC fibers.



Figure 10: Measurement and stabilization of the phase and envelope phase mismatch for frequency combs generated by a femtosecond laser in the mode-locking mode.

Convenient, reliable and compact solid-state femtosecond laser systems, widely used 20 years ago, allow the formation of frequency combs with a spectral extension sufficient for practical use in optical metrology and precision spectroscopy. The intermode interval $\Delta\omega$ can be attached to a radio frequency reference source, such as, for example, an atomic cesium clock. However, even after this procedure, the frequency comb is not yet fully tied to the reference frequency standard. The difficulty lies in the fact that the frequency of the nth spectral component of the frequency comb is not exactly a multiple of the intermode interval $\Delta\omega$, but is determined by the expression $\omega_n = n\Delta\omega + \omega_0$, where $\omega_0$ is the detuning frequency. One of the physical causes of the frequency of detuning is associated with the dispersion of the optical elements of the laser cavity, which leads to a difference in the phase and group velocities $u_p$ and $u_g$. Because of the difference $u_p$ and $u_g$, the phase of the light field is systematically shifted from pulse to pulse in a train radiated by a laser with synchronized modes relative to the envelope of the pulse. As a result, at the output of a femtosecond laser with synchronized modes, a sequence of pulses is formed, separated by identical time intervals T, but having a non-zero detuning $\Delta\varphi$ of the carrier phase and the phase of the light pulse envelope. The Fourier transform of such a field gives the spectrum in the form of an equidistant comb of spectral components (Fig. 10) with frequencies $\omega_n = n\Delta\omega + \omega_0$, where $\omega_0 = \Delta\varphi/T$.

To use a frequency comb as a ruler for high-precision frequency measurement, it is required to measure and stabilize the value of $\omega_0$ by an external reference frequency standard. This problem is solved by generating a supercontinuum in the MS fiber. The

principle of measurement and stabilization of $\omega_0$ is shown in Fig. 10. A portion of the radiation from the femtosecond laser source of the frequency comb is passed through the MS fibers. The other part is used to generate the second harmonic (SHG) in a nonlinear crystal. The key requirement for the supercontinuum generation operation in the MS fiber is that the width of the supercontinuum spectrum at the output of the MC fiber should exceed an octave [22]. If this condition is satisfied for some spectral component $n$ selected in the low-frequency region of the initial comb, the radiation spectrum transformed into the MC fiber will contain a frequency component $\omega_{2n} = 2n\Delta\omega + \omega_0$, which is close in frequency to the component $2\omega_n = 2n\Delta\omega + 2\omega_0$ in the spectrum of the second harmonic signal (Fig. 10). The beat signal of the second harmonic and radiation fields at the output of the MC fiber will thus contain the component $2\omega_n - \omega_{2n} = \omega_0$, allowing to measure and stabilize the detuning frequency $\omega_0$ and, thus, to bind all the spectral components of the femtosecond frequency comb to the reference standard frequency using only one laser source. Optical metrology systems, based on the use of frequency combs, provide relative accuracy of measuring frequency intervals at the level of $5\times10^{-16}$. Due to its simplicity, compactness, and reliability, the technique of femtosecond frequency combs is widely used for measurements of fundamental physical constants and creation of practical optical clock circuits [22]. The possibilities of using such systems for satellite navigation, as well as for high-precision synchronization of optical networks, are actively explored.

## 6.2 Spectroscopy of coherent anti-Stokes light scattering

Coherent anti-Stokes scattering of light (CARS) [23, 24] is one of the most widely used methods of nonlinear spectroscopy. The CARS technique provides high spatial, temporal and spectral resolution for studying excited gas media and plasma, and is also widely used for microscopy of biological objects and ionized spatially inhomogeneous gas media. Femtosecond CARS spectroscopy makes it possible to study fast processes and the dynamics of vibrational wave packets in molecular systems in the gas, liquid, and solid phases. The possibilities of CARS spectroscopy and CARS microscopy, including sensitivity, as well as the temporal, spatial and spectral resolution of these techniques, are substantially broadened by using the methods of polarization and phase control of four-photon scattering processes.

The use of parametric light generators and organic dye lasers as sources of tunable radiation radically expanded the field of applications of CARS spectroscopy, allowing in

many cases to turn the CARS technique from the method of laboratory research into an engineering tool for the practical investigation of automobile and rocket engines.

Spontaneous Raman scattering of light is associated with thermal vibrations of molecules. Light waves and oscillations of the medium mutually influence each other [25]. The reason for the inverse action of the light waves on molecular oscillations is dependency $\chi(\eta_i)$. When a molecule gains a dipole moment in the field of the light wave, it begins to interact with it. The interaction energy:

$$W = -PE = -\chi(\eta_i)E^2. \tag{6.1}$$

Force acting on a molecule:

$$F = -\frac{dW}{d\eta_i} = \frac{d\chi}{d\eta_i}E^2. \tag{6.2}$$

Anti-Stokes scattering is interesting in that there is no luminescence of the sample in the anti-Stokes region. The energy diagram is shown in Fig. 11 [26].
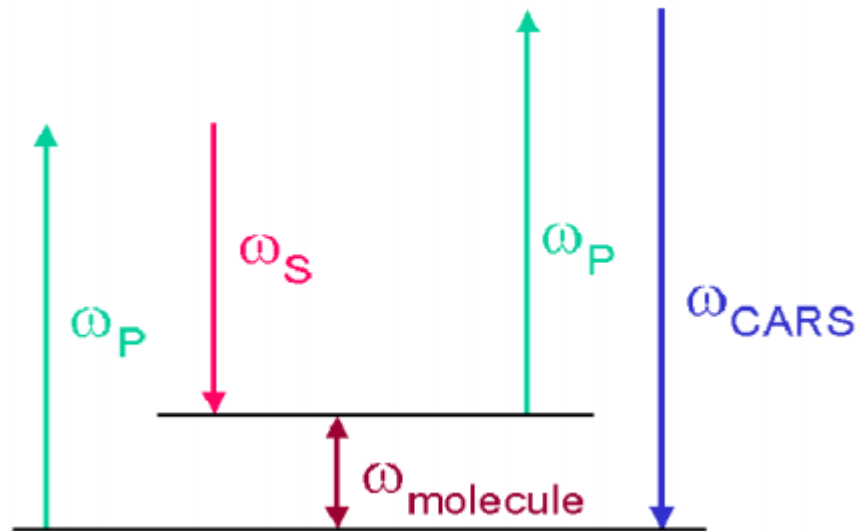


Figure 11: The CARS energy diagram. $\omega_{CARS}$ is the frequency of a probe field, $\omega_{molecule}$ is the frequency of the natural oscillations of a molecule, $\omega_s$ is the frequency of a Stokes field, $\omega_p$ is the frequency of a pump field.

The pump ($\omega$p) and the Stokes ($\omega$S) frequencies form for a beat frequency ($\omega$p-$\omega$S). If the beat frequency coincides with a vibrational resonant frequency of the molecule, the beat signal lifts the molecule to higher vibrational state. The CARS signal at $\omega$p + $\omega$p − $\omega$S is created when a probe pulse at $\omega$p is coherently mixed with the beat signal. The schematic diagram of experiments in CARS spectroscopy is presented below in Figure 12.
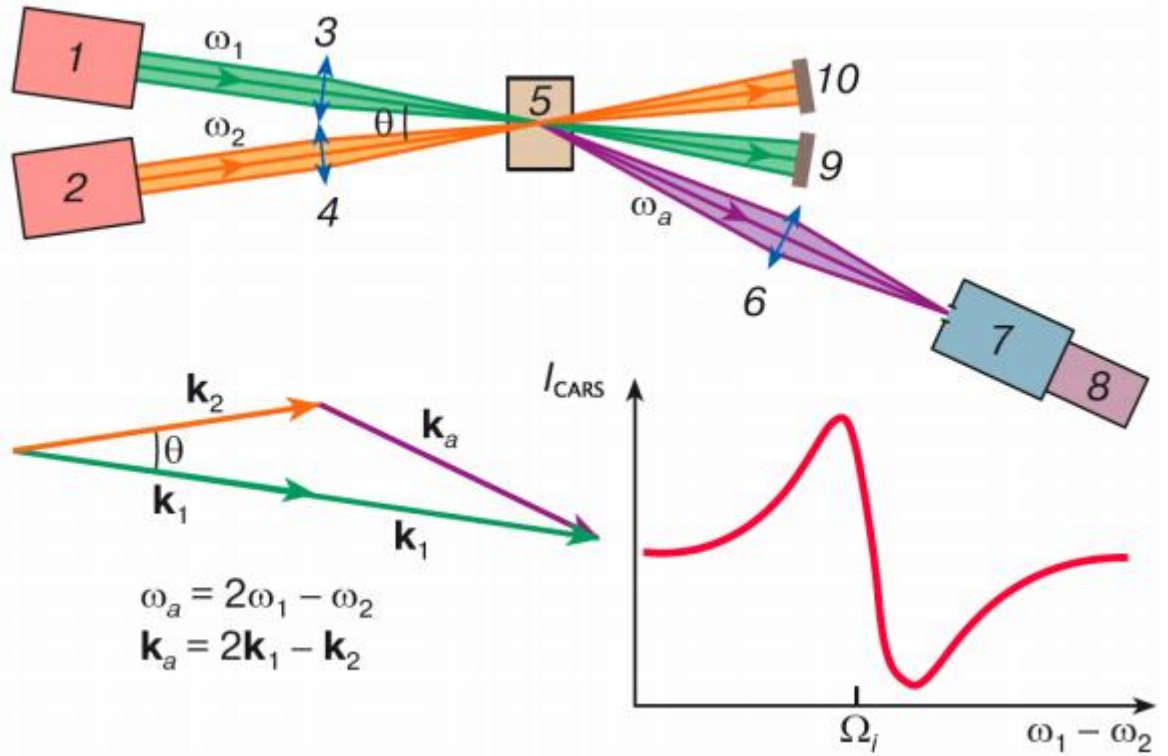
Figure 12: Schematic diagram of CARS spectrometer and common CARS spectrum

In [27], a new scheme of femtosecond CARS spectroscopy based on the use of pulses with phase modulation was proposed and experimentally realized. Linear time-frequency display, determined by pulses with linear phase modulation, allows measuring the spectra of the nonlinear response of a medium by changing the delay time between the pump pulses. The key idea of the experimental implementation of the proposed experimental technique is to use MC fibers with a special dispersion profile to generate frequency-tunable pulses with a smooth envelope and controlled phase modulation. Due to the high degree of localization of electromagnetic radiation in the core and the possibility of forming the desired dispersion profile, the MC fibers can radically increase the efficiency of the nonlinear-optical frequency conversion of femtosecond pulses, opening up the possibility of creating fundamentally new sources of frequency-tunable radiation for nonlinear spectroscopy. The frequency-tunable femtosecond pulses generated in the MS fibers are used to obtain the CARS signal from the toluene solution.

The laser system used in the experiments [27] consisted of a Cr: forsterite, stretcher, an optical isolator, a regenerative amplifier, a compressor and a crystal for doubling the frequency [20] (Fig. 13b). A fiber ytterbium laser was used to pump the master laser. The master laser generated pulses with a characteristic duration of 30 to 50 fs and a repetition rate of 120 MHz. The central wavelength of these pulses was 1270 nm. The average

radiation power of the laser was about 180 mW. The amplification of the femtosecond pulses generated by the master oscillator was performed by means of a regenerative amplifier pumped by the radiation of an Nd: YLF laser. The amplified pulses with energies up to 100 μJ were fed to a lattice compressor, where pulses were compressed to a length of 75 − 150 fs with a loss of approximately half the energy. The frequency of chromium-forsterite laser radiation was doubled with an LBO crystal.
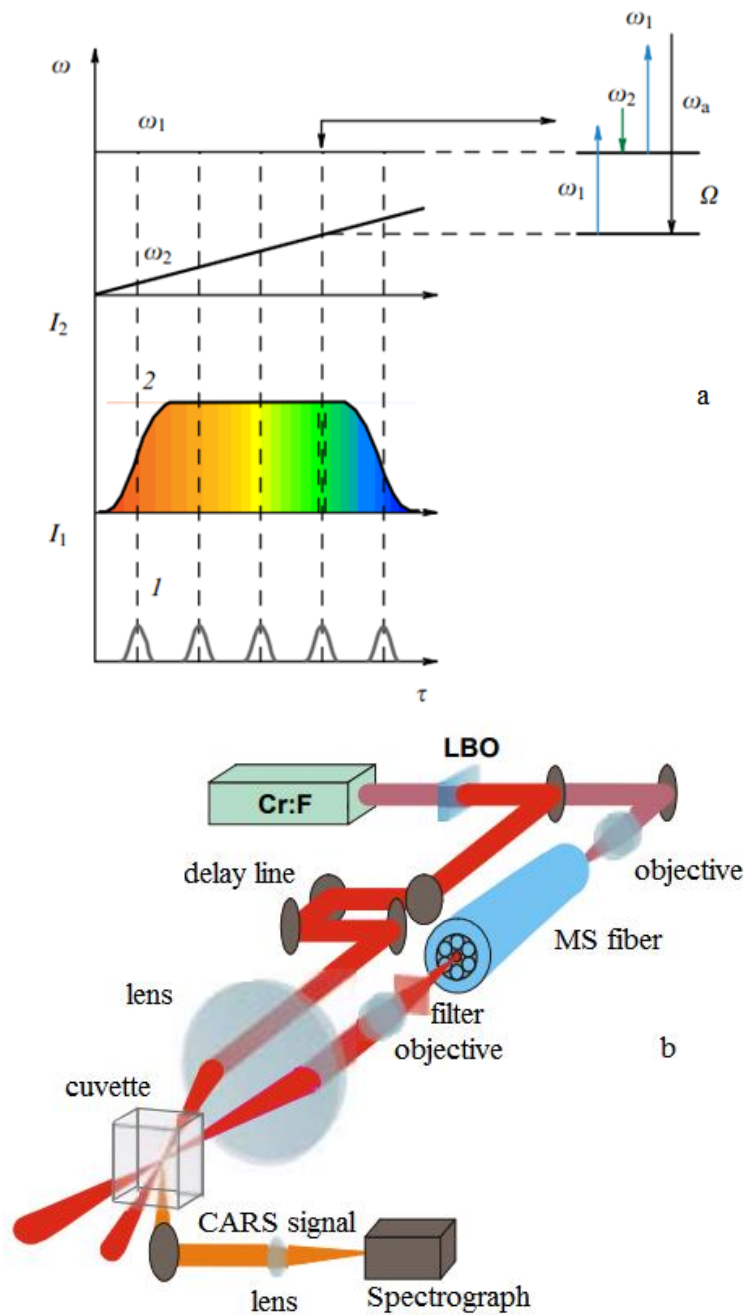


Figure 13: (a) Principle of femtosecond CARS spectroscopy using FM pulses. (b) Scheme of the experimental setup for CARS spectroscopy using FM pulses generated in a MS fiber.

Microstructured fibers were made from multicomponent glass. The fiber structure provided a dispersion profile of the waveguide modes, which makes it possible to achieve the maximum efficiency of converting the energy of laser radiation into a signal shifted to the high-frequency region (anti-Stokes) with a wavelength of 650-730 nm. To measure the duration and chirp of the anti-Stokes signal generated in the MS fiber, we used a cross-correlation technique similar to the XFROG technique (cross-correlation frequency-resolved optical gating) [28]. The XFROG technique is based on measuring the spectrum of the total frequency signal generated by mixing anti-Stokes radiation from the MS fiber and the second harmonic of the chromium forsterite laser in the crystal for different values of the delay time $\tau$ between the second-harmonic pulse $E_{SH}$ and the anti-Stokes signal $E_a$.

The measured spectrogram makes it possible to obtain information on the shape of the envelope, duration, spectrum, and chirp of the anti-Stokes pulse generated in the MS fiber:

$$S(\omega, \tau) \propto \left| \int_{-\infty}^{\infty} E_a(t) E_{SH}(t - \tau) \exp(-i\omega t) \, dt \right|^2. \qquad (6.3)$$

The different frequency components of the anti-Stokes pulse generated in a MS fiber are characterized by different group delays. This allows to make spectral measurements by changing the delay time between the pump pulses. In these anti-Stokes experiments, the signal generated in the MS fiber was used as one of the pump pulses in the CARS spectroscopy scheme.

The second harmonic of the emission of a chromium-forsterite laser with a frequency $\omega_1$ and anti-Stokes signals from the MC fiber (frequency $\omega_2$) was used to excite the Raman-active modes of toluene molecules in a solution with frequencies $\Omega = \omega_1 - \omega_2$. The radiation of the second harmonic of the chromium-forsterite laser scattered by the phased media vibrations led to the appearance of the CARS signal at the frequency $\omega_{CARS} = 2\omega_1 - \omega_2$ . The fiber structure was optimized to efficiently generate an anti-Stokes signal in the frequency range, which allows probing of the combination-active modes of toluene molecules in the region 1000-1200 cm$^{-1}$. The light pump beams with frequencies $\omega_1$ and $\omega_2$ were focused into a cuvette with a solution of toluene at a small angle. The CARS signal was generated in the region of interaction of the pump beams in a cuvette with toluene in the form of a narrow beam, spatially separated from the pump radiation. This signal was separated from the pump beams and recorded with a spectrometer. The change in the delay time $\tau$ corresponds to the change in the instantaneous frequency difference $\omega_1 - \omega_2$, which makes it possible to excite various combinational modes of toluene molecules. At low $\tau$ corresponding to the trailing edge of the anti-Stokes pulse, low-frequency combinational modes are excited. As the delay time

increases, the instantaneous frequency difference $\omega_1 - \omega_2$ increases, which leads to the excitation of combinational modes of higher frequencies.

# 7 Experimental setup and measurements

## 7.1 Assembly and configuration of the experimental setup

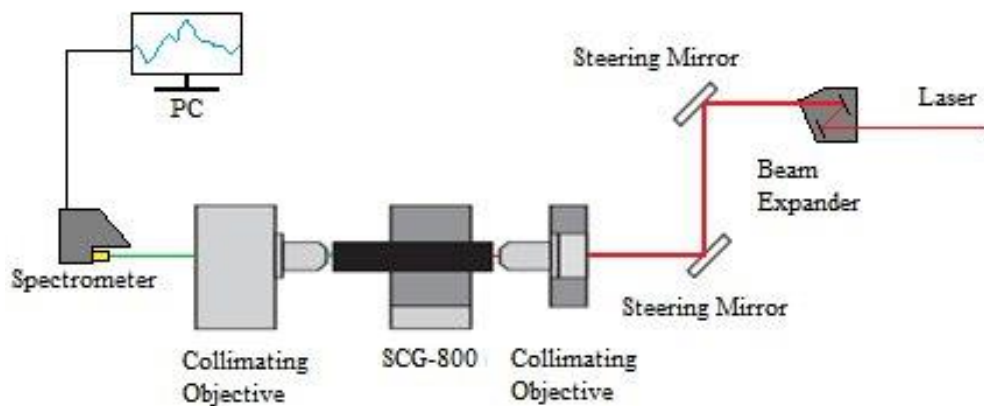Block diagram of the experimental setup is shown in Figure 14.



Figure 14: Block diagram of the experimental setup

Assembly begins with the pumping laser. In this work laser is Toptica MA Femto Fiber pro 11 (Fig. 15). Our laser has two outputs for two different wavelengths of 1560 nm and 780 nm. In this paper, wavelength is 780 nm, which corresponds to the near-infrared (NIR) range. The laser power is 170 mW, pulse duration is 80 fs, and repetition rate is 80 MHz.



Figure 15: The pumping laser

From the laser beam enters the beam expander (Fig. 16) to make the beam wider and non-divergent. This is an important part of the setup and should not be overlooked. To

achieve a high coupling efficiency, the pump beam must be positioned close to normal incidence with respect to the fiber. Then the beam passes through two steering mirrors are used for leveling the beam parallel to the optical table and to the axis of the PCF SCG-800 (Fig. 17).



Figure 16: The beam expander and two mirrors

The holder for SCG-800 is an essential part of the setup. It plays a critical role in the stability and reproducibility of the continuum, given the fact that the core diameter of the SCG-800 is only 1.8 µm. The pump beam is focused into the fiber using a 20x objective. The 20x objective is used after the SCG-800 to collimate the output beam.
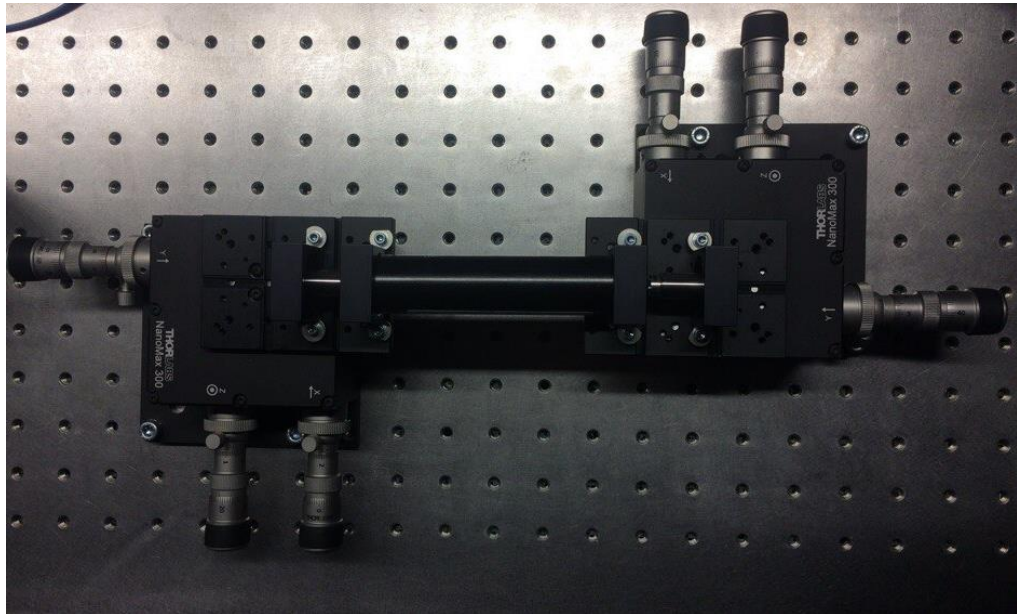
Figure 17: Focusing lens, PCF and collimating lens (from right to left)

Then the collinear ray hits the high-resolution spectrometer (Fig. 17). Main Key Benefits of this spectrometer are high resolution 0,6nm/FWHM, it's less than 0,03% from the stray light, and it's the first work with such a high-resolution for supercontinuum, and wide spectral range 475 – 1100 nm, visible and near-infrared range.



Figure 18: FREEDOM mini Raman 475 – 1100 nm

## 7.2 Measurements

To obtain a supercontinuum, an installation was assembled and each element of the circuit was calibrated. After assembly of the installation, each element must be calibrated until we get a bright red spot from a small point at low power, saying that the beam hits the edge of the core of the PCF (Fig. 19).
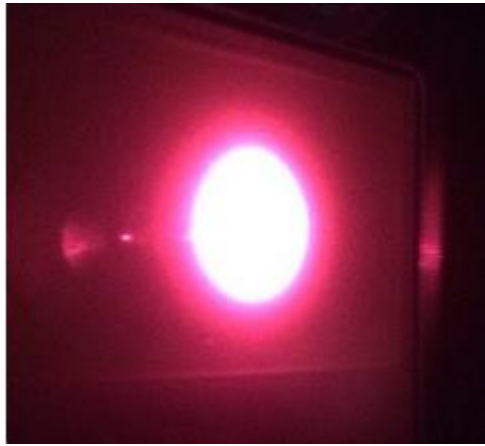
Figure 19: Bright red spot

Next, we need to get to the very center of the photonic crystal fiber. The signal will be a change in color towards short wavelengths, i.e. change of red to yellow or light green (Fig. 20).



Figure 20: Bright yellow spot

For the beginning, we will remove the dark spectrum so that in the future these noises did not affect the result (Fig. 21).
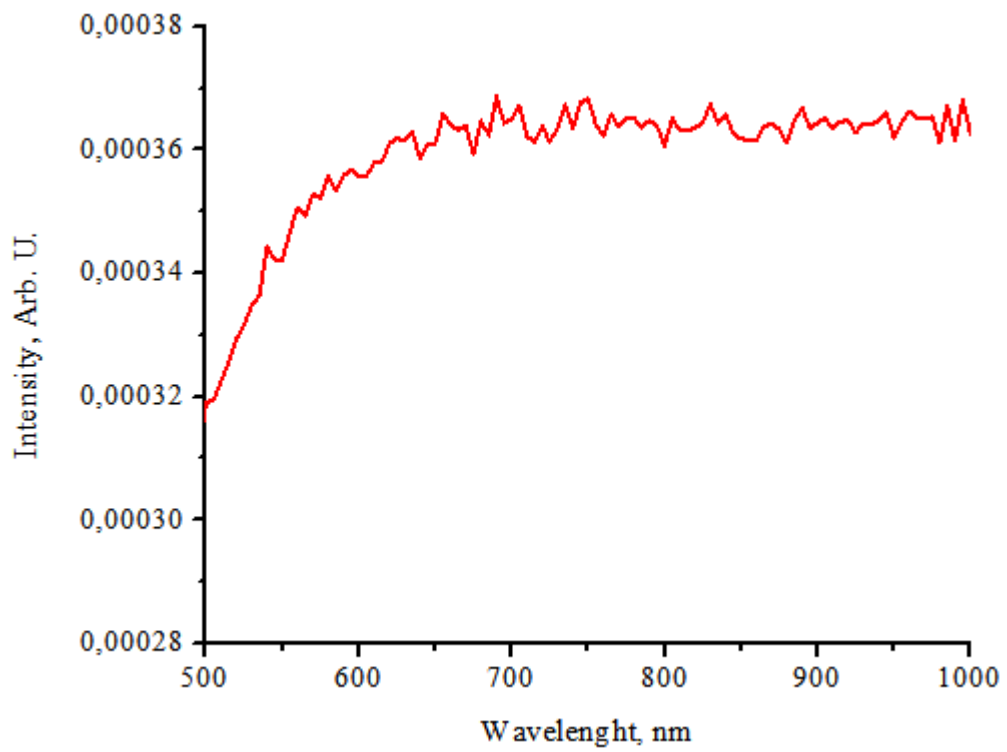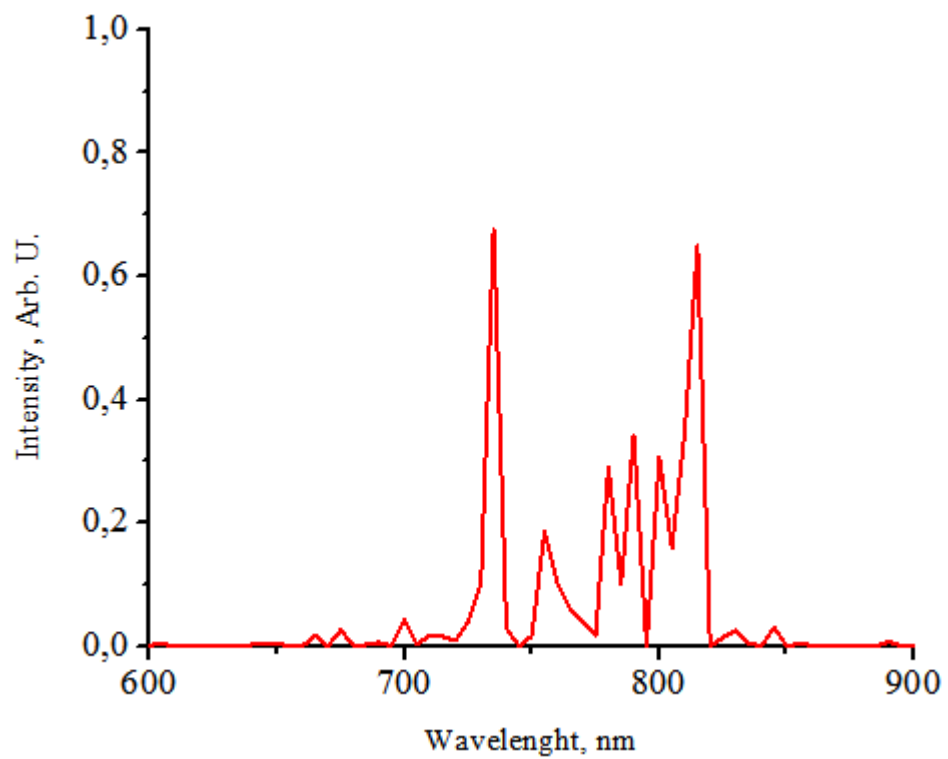
Figure 21: Dark spectrum



Figure 22: 40% of laser power

We can observe a spectrum with a width of 730 nm to 820 nm, which cannot be called a good supercontinuum.
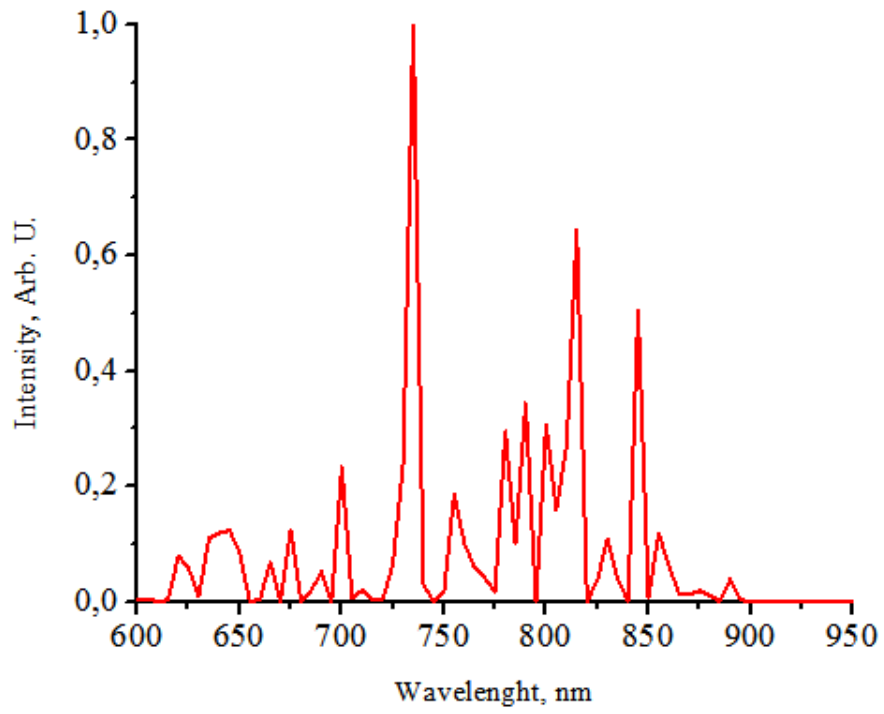
Figure 23: 50% of laser power

Increasing the power by 10%, one immediately sees the broadening of the spectrum and the increase in the radiation intensity.
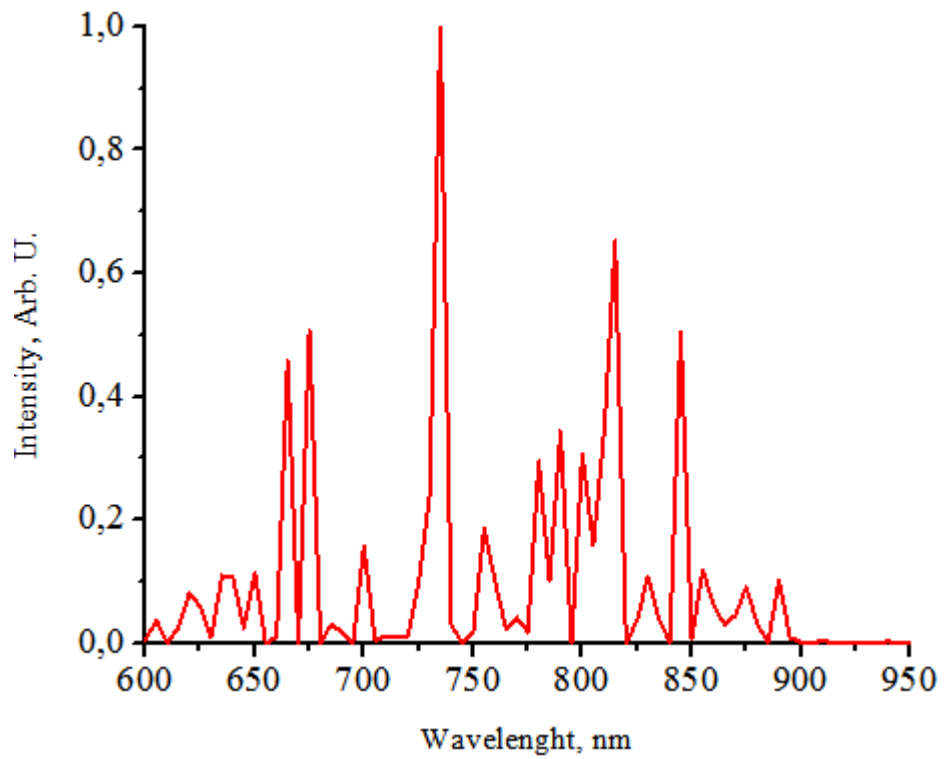


Figure 24: 60% of laser power

Increasing the power by another 10%, we see further the broadening of the spectrum and the increase in the radiation intensity.
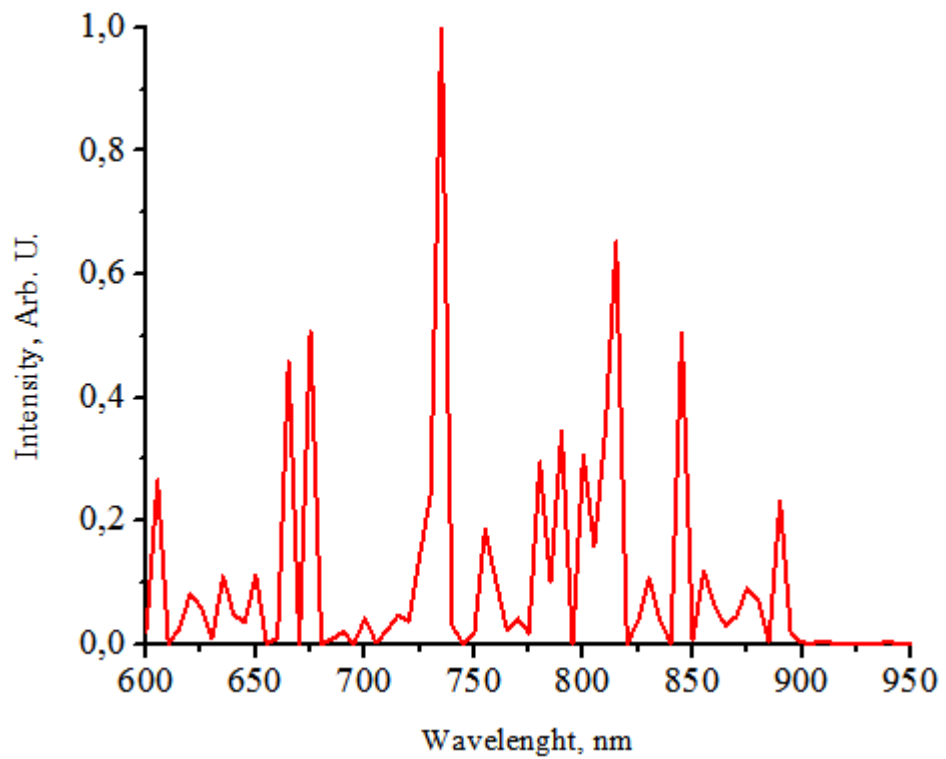
Figure 25: 70% of laser power

Increasing the power by another 10%, we see further the increase in the radiation intensity.
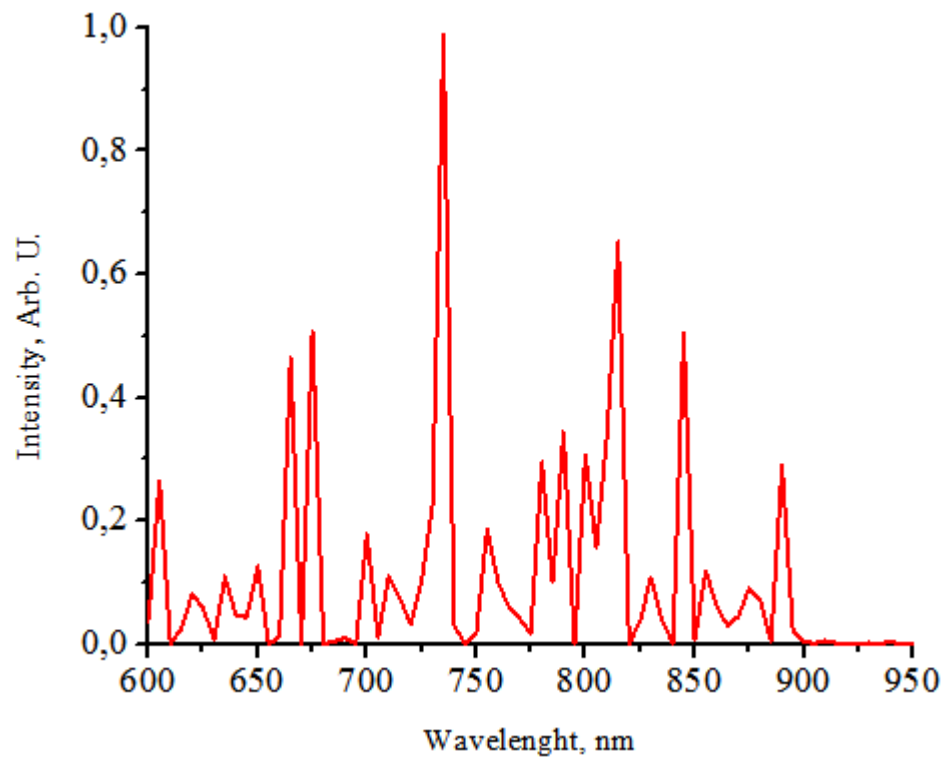


Figure 26: 80% of laser power

49

Increasing the power from 70% to 80%, we see further the increase in the radiation intensity.
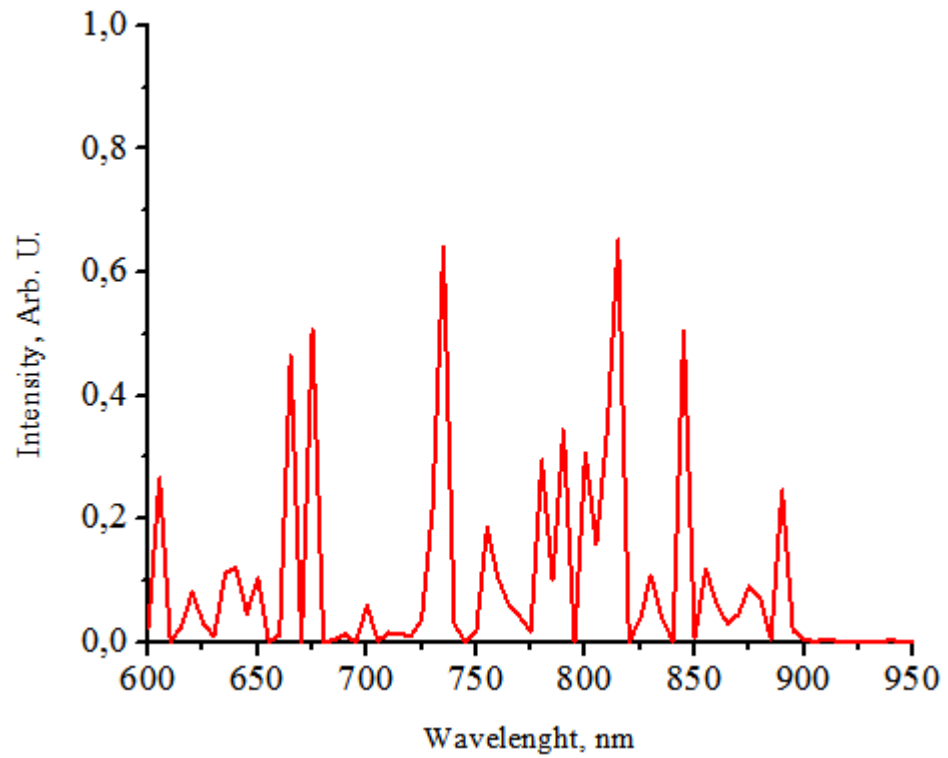


Figure 27: 90% of laser power

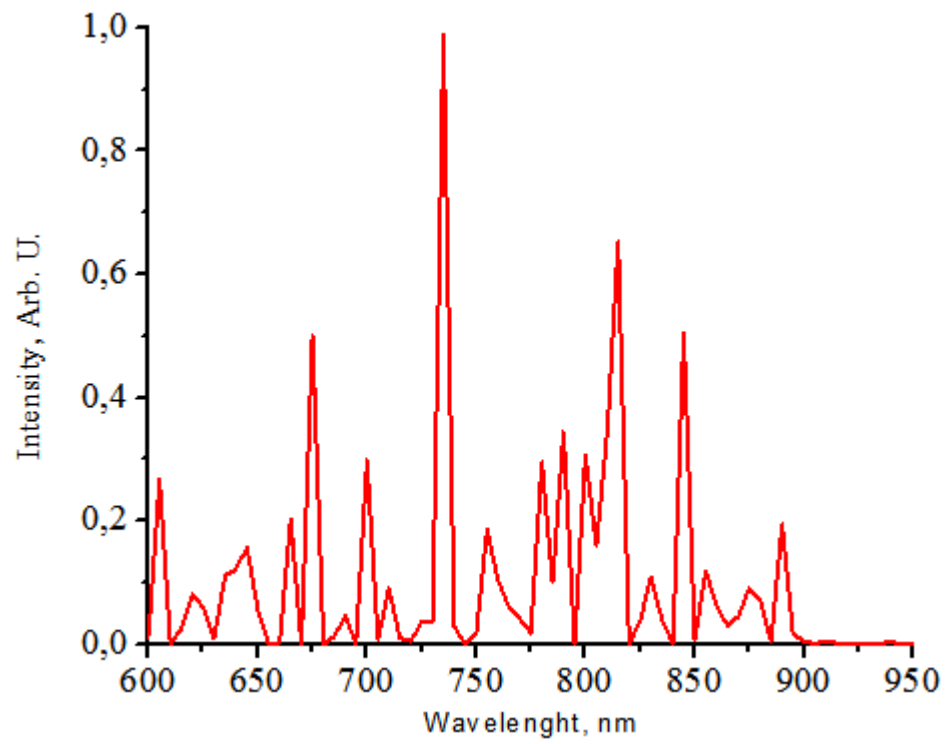Increasing the power from 80% to 90%, we see further the increase in the radiation intensity.

Figure 28: 100% of laser power

Increasing the power from 90% to 100%, we see further the increase in the radiation intensity.

# 8 Conclusions

In this thesis, the properties of the supercontinuum from different laser pumping powers are studied. It is important to study the influence of power on width, on the shape of the spectrum, on the spectral features, so that this can be used in the development of supercontinuum applications, such as CARS spectroscopy.

Depending on the laser power, various forms of the spectrum appear at the fiber exit. It can be assumed that effects such as four-wave interactions and phase self-modulation, cross phase modulation, are responsible for these effects. However, other mechanisms are possible, and therefore the justification for the effect of the appearance of a supercontinuum in a photonic crystal requires additional measurements.

Studies carried out with the help of a high-resolution spectrometer made it possible to determine the width and shape of SC spectra.

In the future, this installation can be used as part of the installation for CARS spectroscopy with a single laser beam. Adding a delay line and selecting the necessary geometric parameters, you can explore different samples. Having assembled such an installation in one box together with the laser, you can immediately start studying various materials without spending a lot of time and money on assembling and purchasing several lasers, since only one laser will be needed, which makes this idea very convenient and necessary in the implementation in scientific and civilian purposes.

# References

[1]     C. V. Raman, K. S. Krishnan, *Nature*, vol.121, p. 501, 1928.

[2]     R. R. Alfano, S. L. Shapiro, *Phys. Rev. Lett*., vol. 24, p. 584, 1970.

[3]     R. R. Alfano, P. L. Baldeck, *Lightwave Technol*., vol. 5, p. 1712, 1987.

[4]     Y. R. Shen, *The principles of nonlinear optics*, New York, 1984.

[5]     T. Brabec, F. Krausz, *Rev. Mod. Phys*., vol. 72, p. 545, 2000.

[6]     S.A. Akhmanov, A.S. Chirkin, *Optics of femtosecond laser pulses*, Moscow: Science, 1988.

[7]     G. P. Agrawal, *Nonlinear Fiber Optics*, 3rd ed., San Diego, CA: Academic, 2001.

[8]     G. Mejean  et al., *Appl. Phys.,* vol. 77, p. 357, 2003.

[9]     K. R. Tamura, H. Kubota, M. Nakazawa, *IEEE J. Quantum Electron*., vol. 36, p. 773, 2000.

[10]     P. St. Russell, *Science*, vol. 299, p. 358, 2003.

[11]     C. M. Smith, N. Venkataraman, M.T. Gallagher, D. Muller, J. A. West, N.F. Borrelli, D.C. Allan, K. Koch, *Nature*, vol. 424, p. 657, 2003.

[12]     A.M. Zheltikov, *Successes of physical sciences*, vol. 174, p. 73, 2004.

[13]     J. K. Ranka, R.S. Windeler, A. J. Stentz, *Opt. Lett*., vol. 25, p. 25, 2000.

[14]     W. J. Wadsworth et al.,  *J. Opt. Soc. Am*., vol. 19, p. 2148, 2002.

[15]     S. Coen, A. H. Chau, R. Leonhardt, J. D. Harvey, J.C. Knight, W. J. Wadsworth, P. St. Russell *J. Opt. Soc. Am*., vol. 19, p. 753, 2002.

[16]     J. B. Jensen, L. H. Pedersen, P. E. Hoiby, L. B. Nielsen, T. P. Hansen, J. R. Folkenberg, J. Riishede, D. Noordegraaf, K. Nielsen, A. Carlsen, A. Bjarklev, *Opt. Lett.,* vol. 29, 2004.

[17]     S. O. Konorov, A. Zheltikov, M. Scalora, *Opt. Express*, vol. 13, 2005.

[18]     A. B. Fedotov, S. O. Konorov, E. E. Serebryannikov, D. A. Sidorov-Biryukov, V. P. Mitrokhin, K. V. Dukelískii, A. V. Khokhlov, *Opt. Commun*., 2005.

[19]     G. P. Agrawal, *Phys. Rev. Lett.*, vol. 59, p. 880, 1987.

[20]     A. Zheltikov, *Successes of physical sciences*, vol. 174, p. 743, 2004.

[21]     J. N. Eckstein, A. I. Ferguson, *Phys. Rev. Lett.*, vol. 40, p. 847, 1978.

[22]     T. Udem, R. Holzwarth, T. W. Hansch, *Nature*, vol. 416, p. 233, 2002.

[23]     G. L. Eesley, *Coherent Raman Spectroscopy*, Oxford, 1981.

[24]     S. A. Akhmanov, N. I. Koroteev, *Nonlinear optics methods in light scattering*

*spectroscopy*, Moscow, 1981.

[25]    N. B. Delone, Nonlinear optics, *Soros Educational Journal*, vol .3, pp. 94-99, 1997.

[26]    W. Hubschmid, R. Bombach, *Laser spectroscopy in combustion research*, 2002.

[27]    S. O. Konorov, D. A. Akimov, A. A. Ivanov, M. V. Alfimov, *Appl. Phys.*, vol. 78, p. 565, 2004.

[28]    R. Trebino, *Frequency-Resolved Optical Gating: The Measurement of Ultrashort Laser Pulses,* Boston, 2002.